PHYSICAL SETTING

John Schoen

PHYSICAL SETTING MAP INDEX

MAP ON PAGES 20–21

Ocean Currents

Erika Knight and Skye Cooley

Ocean currents are continuous, directed movements of ocean water masses that flow at local or global scales at the ocean surface or at depth (National Oceanic and Atmospheric Administration 2017). Current movement is driven by a variety of factors, such as wind forcing, water density, tidal influence, and the Coriolis Effect—an inertial force generated by the Earth's rotation that deflects ocean currents (and weather) to the right in the Northern Hemisphere, and to the left in the Southern Hemisphere. Currents can also be driven by sea-level differences. For example, northward transport of Pacific Ocean water through the Bering Strait is driven by a sea-level difference of approximately 1.3 feet (0.4 m) between the Bering Sea and Arctic Ocean (Stabeno et al. 1999).

Each ocean current has similar properties—temperature, salinity, carbon, nutrients, and bioproductivity of organisms—that impart a distinct signature to the water mass (Weingartner et al. 2012). Taken together, this group of properties influences how water masses interact with each other. Water density is dependent upon temperature and salinity; therefore the freshwater content of ocean current flow through the Bering Strait influences where this water is transported as it enters the Arctic Ocean (Weingartner 2008). Due in part to the many major rivers that drain the fresh waters of central Alaska westward into the Bering Sea, flow from the Bering Strait into the Arctic Ocean "provides nearly 50% of the total freshwater input to the Arctic Ocean," making it the largest source of fresh water for the Arctic Ocean (Weingartner 2008).

Due to the distinct properties of each water mass, the vertical lifting of bottom water to the surface, known as upwelling, is an important phenomenon associated with high bioproductivity. Upwelled water is often characterized by its relatively low temperature, high salinity, and high nutrient content. When this water is brought to the ocean surface, often via the movement of ocean currents onto a continental shelf, or by winds pushing surface water away so deeper waters rise to replace the surface-water void, it fuels productivity, which forms the energy base for higher trophic-level consumers (National Oceanic and Atmospheric Administration 2017).

Ocean currents can have a profound effect on sea ice. Likewise, sea ice also affects ocean currents. Pacific Ocean waters transport heat into upper levels of the Arctic Ocean, providing up to 20% of the oceanic heat flux (Weingartner 2008). This transported, warmer water likely plays an important role in the recent retreat of Arctic sea ice, both as a trigger for seasonal sea-ice melt and as a year-round warming agent that may thin the Arctic ice pack in winter (Weingartner 2008, Woodgate et al. 2010). In turn, the formation of sea ice can drive flow. When seawater freezes into ice, the salt remains in the surrounding water through a process called brine rejection, causing the water to become saltier and denser and sink toward the ocean bottom (National Oceanic and Atmospheric Administration 2017). Surface water flows in to replace the sinking water before it, too, becomes colder and salty enough to sink in a process referred to as thermohaline circulation (National Oceanic and Atmospheric Administration 2017). These ocean current / sea ice interactions, combined with seasonal weather patterns, contribute to a dynamic and seasonally variable circulation pattern in the Bering, Chukchi, and Beaufort Seas.

SETTING

Water flows into the Bering Sea from the Pacific Ocean primarily through Near Strait, at the western end of the Aleutian Islands. Farther west, deep water from the Pacific enters the Bering Sea at depths greater than 6,500 feet (2,000 m) through the Kamchatka Strait, the only underwater pass into the Bering Sea deep enough to permit this deep Pacific water to enter (Stabeno et al. 1999). More water from the Pacific enters the Bering Sea through other passes in the Aleutian Islands.

Within the Bering Sea, water circulates in a counter-clockwise pattern, referred to as the Bering Gyre, with some water exiting the Bering Sea via the shallower (less than 4,900 feet [1,500 m]) portion of Kamchatka Strait, and some leaving the Bering Gyre to flow northward toward the Bering Strait. Local transport volume of the gyre varies widely—up to approximately 50%—with variations associated with the inflow of the Alaskan Stream current and with changes in wind-driven transport through the Bering Strait (Stabeno et al. 1999).

Flow through the Bering Strait is largely driven by an approximate mean sea-level difference of 1.3 feet (0.4 m) between the Bering Sea and Arctic Ocean (Stabeno et al. 1999). The volume and properties of water flowing through the Bering Strait influences physical and biogeochemical properties throughout much of the northern Bering shelf; the high productivity of the southern Chukchi Sea is sustained by the low salinity, nutrient-rich waters flowing into the Chukchi Sea from the Bering Strait (Weingartner 2008).

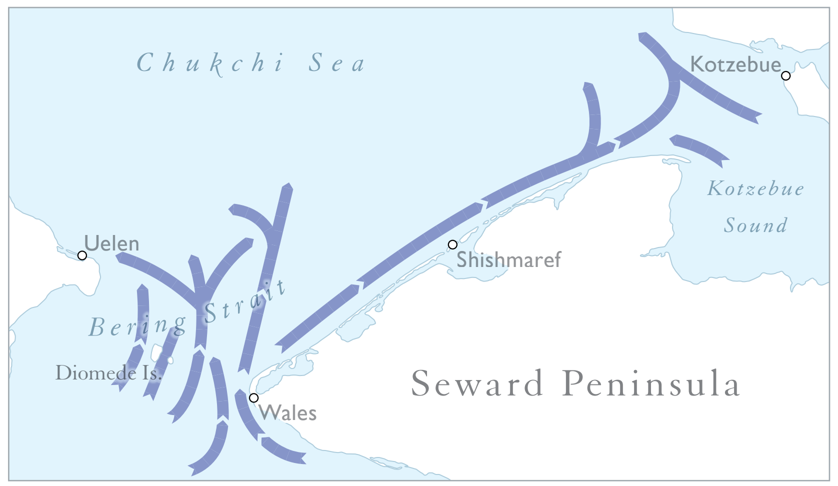

FIGURE 2.1-1. Ocean currents in the Bering Strait region, generalized from traditional knowledge of Bering Strait ocean currents documented by Kawerak, Inc. in Raymond-Yakoubian et al. (2014).

North of the Bering Strait, water flows in three main branches (see Map 2.1). A western, cold, salty, nutrient-rich branch, largely the continuation of the Anadyr Current, exits the Chukchi Shelf through Herald Canyon. An eastern, relatively lower-nutrient and lower-salinity branch, a continuation of the Alaska Coastal Current, continues northeastward along the Alaska coastline toward Barrow Canyon. The third branch of Bering shelf water flows northward through the Central Channel between the other two branches before splitting, with some water exiting the shelf into the Canada Basin, and some water flowing eastward to join the Alaska Coastal Current in Barrow Canyon (Weingartner 2008, Weingartner et al. 2013). In the western portion of the Chukchi Sea, along the northern coast of Chukotka, the Siberian Coastal Current flows onto the Chukchi shelf from the East Siberian Sea. North of the Bering Strait, this water mixes with waters flowing northward through the Strait from the Bering Sea (Weingartner 2008, Weingartner et al. 2013). Variability in flow across the Chukchi shelf is principally caused by wind forcing, which is especially influential in fall and winter. During these seasons, winds can redistribute flow from one branch to another or reverse the flow entirely (Weingartner 2008).

Pacific Ocean waters, modified by traveling across the Bering and Chukchi shelves, split after exiting the Chukchi shelf via Barrow Canyon. Some water travels west, perhaps carried by the newly discovered Chukchi Slope Current (Pickart and Corlett 2016). Some water is caught in eddies that spin into the Arctic Basin, and some continues eastward from the Canyon along the Beaufort shelf break (Weingartner 2008, Nikolopoulos et al. 2009). Eastward flow along the Beaufort shelf (often referred to as the Shelfbreak Jet or Beaufort Undercurrent) is

MAP ON PAGES 20–21

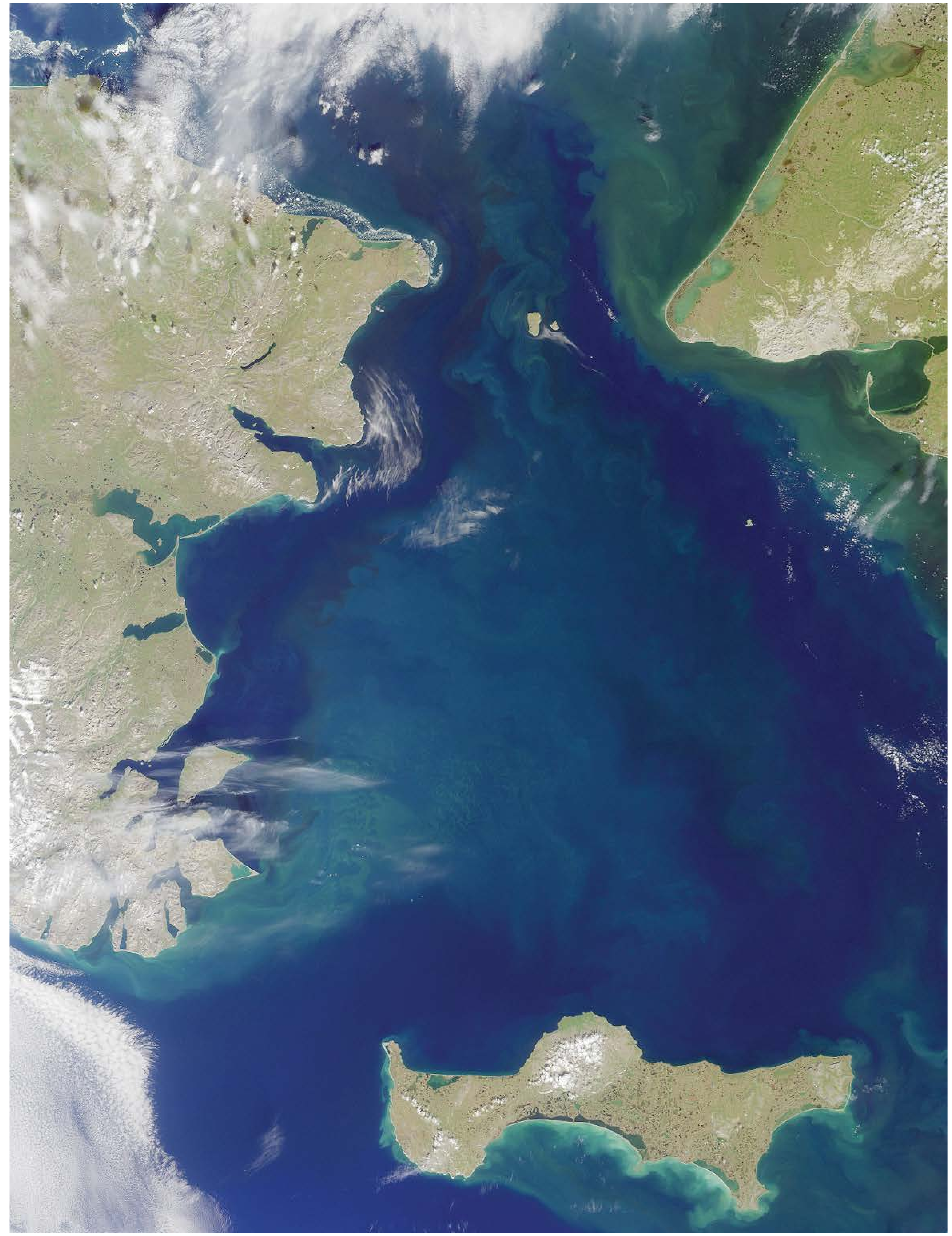

NASA

This view of the Bering Strait region was captured on August 18, 2000. The Anadyr, Bering Shelf, and Alaska Coastal Currents are visible as they converge and carry productivity north through the Bering Strait.

subject to frequent, wind-driven upwelling due to prevailing winds from the northeast and is highly variable, with numerous eddies and changes in flow due to pack ice and landfast ice conditions and inflow from the Mackenzie River. Water properties vary seasonally, controlled in part by freshwater inflows from smaller Arctic rivers along the Beaufort coast, which tend to have high discharge in the spring thaw, but no measurable winter discharge (Weingartner 2008).

ECOLOGICAL ROLE

Alaska Coastal Current
The Alaska Coastal Current, a year-round, wind- and buoyancy-driven jet, flows northward along the inner shelf passages of Southeast Alaska before turning west along the south coast of mainland Alaska and eastern Aleutian Islands (Weingartner et al. 2005b). The Alaska Coastal Current enters the Bering Sea through Unimak Pass (Stabeno et al. 1999), delivering Pacific-origin zooplankton seasonally to the Bering Sea (Weingartner et al. 2005b). Upon entering the southern Bering Sea, a portion of the current turns to the northwest and moves across the Bering shelf (Stabeno et al. 1999). The main current swings abruptly east and north (Grebmeier et al. 2015). As it flows north along the coast of Alaska, the Alaska Coastal Current collects fresh, buoyant, low-nutrient water discharged from large rivers—including the Nushagak, Kvichak, Kuskokwim, Yukon, Kobuk, and Noatak—that drain central Alaska (Arctic Monitoring and Assessment Programme 1998). The Alaska Coastal Current delivers its water to the Chukchi Sea via the Bering Strait and eventually exits the Chukchi Sea via Barrow Canyon (Weingartner et al. 2013).

Alaskan Stream
The Alaskan Stream is the name given to a westward-flowing current that provides the majority of water entering the Bering Sea from the Pacific Ocean. The current begins in the Gulf of Alaska and flows westward along the Aleutian Arc, where it enters the Bering Sea through several passages in the island chain, including Unimak Pass, Amutka Pass, Amchitka Pass, and Near Strait (Reed and Stabeno 1997, Stabeno et al. 1999, Grebmeier et al. 2015). It forms the northern boundary of the counterclockwise North Pacific Gyre. While it is depicted as both independent of and contiguous with the Alaska Coastal Current along the Alaska Peninsula, the Alaskan Stream is distinctly separate from the Alaska Coastal Current west of Amutka Pass. It is a narrow, fast current that generally maintains its position year-round (Reed and Stabeno 1997, Stabeno et al. 1999).

Aleutian North Slope Current
This current, some 12 miles (20 km) wide with a total transport of 3 x 10^6 m^3/s to 5.5 x 10^6 m^3/s, flows on an eastward course along the northern side of the Aleutian Islands. The current originates from water flowing into the Bering Sea through Amchitka and Amukta Passes and feeds the Bering Slope Current (Stabeno et al. 1999).

Anadyr Current
The Anadyr Current begins along the Siberian coast at the northern end of the Bering shelf break. This surface current brings warm, salty, nutrient-rich water from the central Bering shelf eastward through the Gulf of Anadyr, then northward through Bering Strait and into the Chukchi Sea (Nihoul et al. 1993, Stabeno et al. 1999). Water generally exits to the Arctic Basin via Herald Canyon, although some may spread across the Chukchi shelf (Weingartner 2008). The nutrient-rich waters of this current drive high primary productivity in the northern Bering and Chukchi Seas (Nihoul et al. 1993, Weingartner et al. 2013). Flow is generally stable and is greatest in summer. Winter variations are not well understood.

Arctic Circumpolar Boundary Current
Although primarily located outside the map area, the Arctic Circumpolar Boundary Current circulates Atlantic Ocean water through the Arctic Basin into the western Chukchi Sea along the shelf break north of Wrangel Island. The current flows eastward toward the northwest coast of Alaska, where the majority of this Atlantic water continues to flow along the Beaufort slope (Weingartner 2006, Aksenov et al. 2011).

Bering Slope Current
The Bering Slope Current (3 x 10^6 m^3/s to 6 x 10^6 m^3/s) forms the eastern boundary of the Bering Gyre, carrying water from the Aleutian North Slope Current and Alaska Coastal Current northwest across the Bering Sea along the Bering shelf break (Stabeno et al. 1999). As the Bering Slope Current flows along the shelf break, its flow is disrupted and complicated by several large canyons. The current is broken into large eddies (approximately 60 miles [100 km] in diameter) that carry nutrients across the shelf in both directions, increasing primary productivity in the region (Stabeno et al. 1999). At the northern end of the shelf break near Cape Navarin, the Bering Slope Current divides into the westward-flowing Kamchatka Current and the eastward-flowing Anadyr Current (Stabeno et al. 1999, Grebmeier et al. 2015).

Bering Shelf Water (Central Channel)
North of St. Lawrence Island, the Central Channel flows north across the Chukchi shelf and into the Canada Basin. The current carries productive, shelf-modified (low salinity, nutrient-rich) Pacific water into the Chukchi Sea. Reversals of the northward flow occur during periods of strong southward winds, which occur primarily in fall and winter (Stabeno et al. 1999).

Commander Current
Most of the inflow into the Bering Sea through Near Strait turns eastward, forming the Commander Current, which flows along the north side of the Aleutian Island chain, gathering inflow from other passes. East of Amchitka Pass, this current is referred to as the Aleutian North Slope Current (Arctic Monitoring and Assessment Programme 1998).

Kamchatka Current
The Kamchatka Current (7 x 10^6 m^3/s to 15 x 10^6 m^3/s) begins at Cape Navarin, where the Bering Slope Current terminates. Forming the western boundary current of the Bering Gyre, the current flows southward along the Siberian coast (Stabeno et al. 1999). The Kamchatka Current generally flows across Shirshov Ridge and out of the Bering Sea through Kamchatka Strait, re-entering the North Pacific where it contributes to the southbound Oyashio Current; however, at times, a portion of the Kamchatka Current recirculates in the Bering Sea rather than flowing through Kamchatka Strait. Beneath the Kamchatka Current in Kamchatka Strait, deep Pacific water enters the Bering Sea (Stabeno et al. 1999).

Shelfbreak Jet/Beaufort Undercurrent
The Shelfbreak Jet, or Beaufort Undercurrent (approximately 0.13 x 10^6 m^3/s), flows east in a narrow 6–9 mile (10–15 km) swath along the shallow Beaufort shelf, turning northeast at Mackenzie Delta and moving along the Canadian Arctic islands (Nikolopoulos et al. 2009). The jet carries water from the Alaska Coastal Current, which brings North Pacific water through the Bering Strait and onto the Beaufort shelf. However, studies indicate that less than 20% of water passing through the Bering Strait enters the Shelfbreak Jet, depending on several factors including the season, presence of sea ice, and vertical structure of the water column over the shelf (Nikolopoulos et al. 2009). Near Barrow Canyon, eddies form and spin into the Arctic Basin, a phenomenon that may explain the loss of Chukchi-Bering water from the Beaufort shelf. In summer, terrestrial inputs from the Mackenzie River contribute to large, nutrient-rich surface plumes that move both east and west along the Beaufort shelf. Terrestrial sediment inputs from the many rivers along the Beaufort coast are an important source of carbon to nearshore Beaufort shelf regions (Dunton et al. 2012). In the fall and winter, strong easterly winds can temporarily reverse the flow of the Shelfbreak Jet and mix the water column, causing upwelling (Nikolopoulos et al. 2009, Pickart et al. 2011).

Siberian Coastal Current
The Siberian Coastal Current transports cold, low-salinity, nutrient-poor water that originates on the East Siberian shelf to the southeast along the northern coast of Chukotka. The current stays within approximately 37 miles (60 km) of the shoreline before turning northward at the Bering Strait to mix with Bering Strait waters. In some years, winds along the Chukotkan coast prevent the Siberian Coastal Current from entering the Chukchi Sea (Weingartner 2008).

Image and caption by: NASA Earth Observatory (Jesse Allen and Robert Simmon) using Landsat data provided by USGS.

The Yukon River originates in British Columbia, Canada, and flows through Yukon Territory before entering Alaska. In southwestern Alaska, the Yukon Delta spreads out in a vast tundra plain, where the Yukon and Kuskokwim Rivers meander toward the Bering Sea. This natural-color image of the Yukon Delta on September 22, 2002, looks a little like branching and overlapping blood vessels. The rivers and streams flow through circuitous channels toward the sea, passing and feeding a multitude of coastal ponds and lakes. The Yukon Delta is an important habitat for waterfowl and migratory birds, and most of the protected refuge is less than 100 feet (30 m) above sea level. Over such low-lying, mostly treeless terrain, the rivers can change course frequently and carve new channels to find the fastest route toward the sea. The pale color of the sea water around the delta testifies to the heavy sediment load carried by the rivers. People have lived here for thousands of years, and the Yukon Delta is one of Alaska's most populated rural areas, home to thousands of Yup'ik people.

CONSERVATION ISSUES

Ocean currents are important for both humans and marine life. In addition to influencing sea-ice conditions through the transport of heat to the Arctic Ocean (Woodgate et al. 2010), currents transport nutrients and zooplankton to the region. Along with upwelling, this nutrient transport influences the distribution of marine resources such as fishes, birds, and marine mammals. Seabirds, for example, congregate in Aleutian passes where water masses frequently converge and mix (Ladd et al. 2005). On the Bering shelf, pelagic seabird species tend to treat water masses as separate habitat types (Elphick and Hunt 1993). Areas with frequent upwelling events, such as the eastern Beaufort Sea, near Liverpool Bay and the community of Tuktoyaktuk, are often important feeding areas for bowhead whales and other marine mammals, as well as marine birds (Walkusz et al. 2012).

While ocean currents play a major role in the distribution of marine resources, which is important for human activities such as commercial fishing and subsistence hunting, they also affect navigation, safety, and boat travel at both the regional level (e.g. shipping) and local level (e.g., subsistence hunting) (National Oceanic and Atmospheric Administration 2017). Kawerak, for example, has documented traditional knowledge regarding ocean currents in the Bering Strait region, including information about characteristics and locations of currents, use of currents for travel and hunting, and changes to currents (Raymond-Yakoubian et al. 2014).

As oil-and-gas activity and shipping increase in the Arctic, the likelihood of a spill also increases. Knowledge of ocean currents is an important aspect of predicting where spilled hazardous materials may be transported.

MAPPING METHODS (MAP 2.1)

This map shows a generalized representation of typical surface flow patterns across the project area, with deep circulation noted where known. Terrestrial influence on ocean currents is depicted by indicating inputs of fresh water and terrestrial organic matter.

Ocean current data were compiled from several publications including Aksenov et al. (2011), Arctic Monitoring and Assessment Programme (1998), Brugler et al. (2014), Coachman et al. (1975), Grebmeier et al. (2015), Pickart and Corlett (2016), Pisareva et al. (2015), Spall et al. (2008), Stabeno et al. (1999), Takahashi et al. (2011), University of Alaska Fairbanks Institute of Marine Science (2009), Weingartner (2006), Weingartner et al. (2005a), and Weingartner et al. (2005b), as well as based on personal communication with oceanographers Seth Danielson and Phyllis Stabeno.

Locations where upwelling frequently occurs were compiled from Llinás et al. (2009), Pickart et al. (2009), Pickart et al. (2013), Sapozhnikov et al. (2011), and Walkusz et al. (2012).

Because of the importance of terrestrial inputs of fresh water and dissolved and particulate carbon and nitrogen to ocean ecosystems (e.g. Dunton et al. (2012), McClelland et al. (2016)), we have shown annual average discharge of major rivers. These data are based on US Geological Survey streamflow data from gauging stations as close to river mouths as available (US Geological Survey 2016) and annual discharges published in Benke and Cushing (2005). In addition, we have shown interpolated measurements of ^{13}C depletion—an indication of terrestrial versus marine carbon—in sediments across the Beaufort and Chukchi shelves (Dunton et al. 2012). Sediment sampling data from Dunton et al. (2012) were interpolated by Audubon Alaska (2016a) using the inverse distance weighted tool in ArcGIS 10.3 Spatial Analyst with a power of one and nine nearest neighbors.

Data Quality
The generalized approach to displaying ocean current data on this map means that seasonal shifts in the positions of currents, as well as local flow variations, were omitted to preserve clarity at the scale of the entire map. The generalized surface current data are comprehensive across the project area. Deep circulation, however, is less well understood and information on this map is incomplete. Upwelling is shown in areas where it is known to commonly occur; upwelling likely also occurs in areas not depicted on the map. The $\delta^{13}C$ sediment data cover the Beaufort and Chukchi shelves but were unavailable for other portions of the map.

Reviewer
• Tom Weingartner

MAP DATA SOURCES

Ocean Currents: Aksenov et al. (2011); Arctic Monitoring and Assessment Programme (1998); Brugler et al. (2014); Coachman et al. (1975); Grebmeier et al. (2015); P. Stabeno (pers. comm.); Pickart and Corlett (2016); Pisareva et al. (2015); S. Danielson (pers. comm.); Spall et al. (2008); Stabeno et al. (1999); Takahashi et al. (2011); University of Alaska Fairbanks Institute of Marine Science (2009); Weingartner (2006); Weingartner et al. (2005a, b)

Upwelling: Llinás et al. (2009); Pickart et al. (2009, 2013); Sapozhnikov et al. (2011); Walkusz et al. (2012)

^{13}C Depletion in Sediments: Audubon Alaska (2016a) based on Dunton et al. (2012)

Ocean Currents

Map Authors: Skye Cooley, Erika Knight, and Melanie Smith
Cartographer: Daniel P. Huffman

Audubon ALASKA

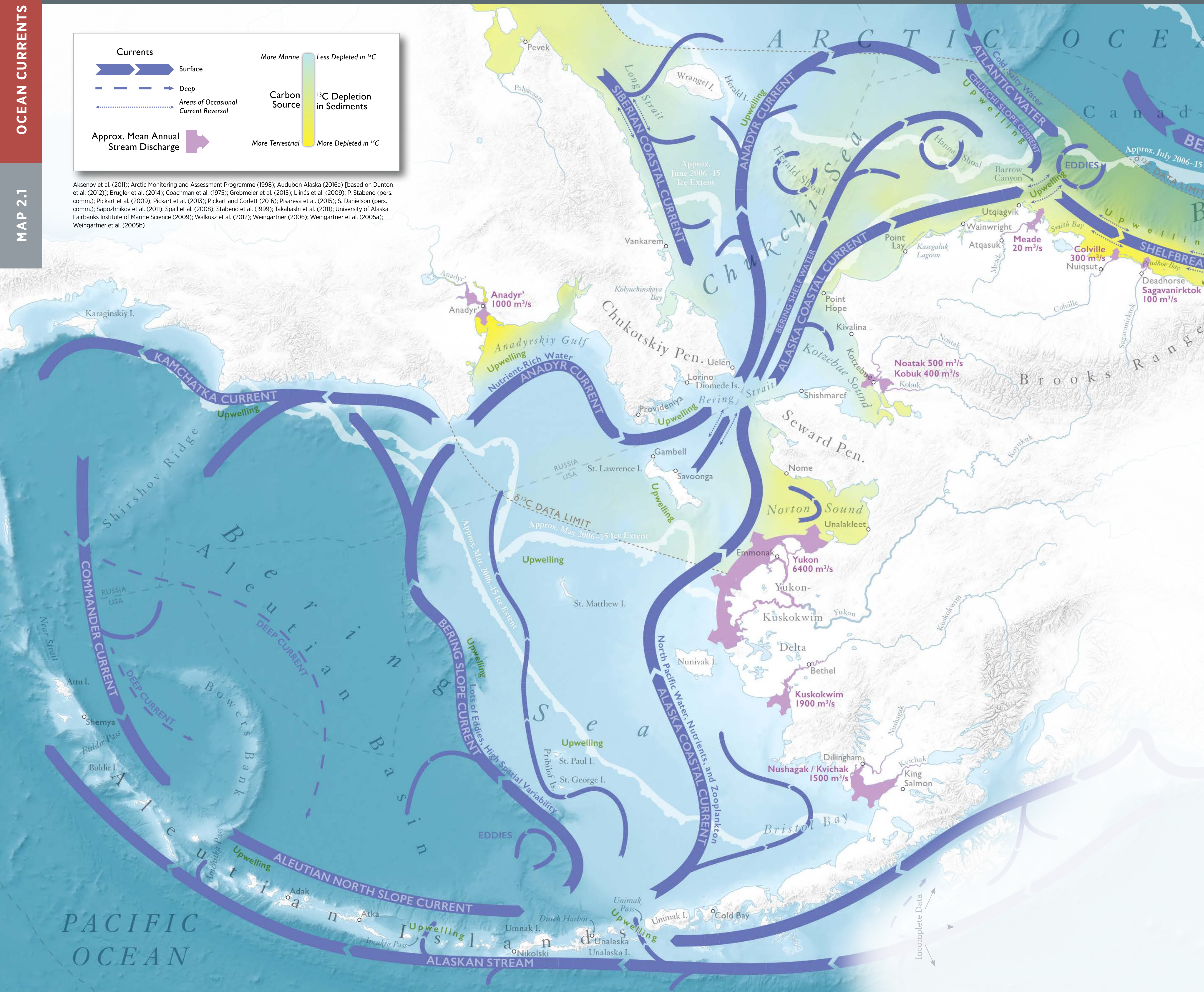

Aksenov et al. (2011); Arctic Monitoring and Assessment Programme (1998); Audubon Alaska (2016a) [based on Dunton et al. (2012)]; Brugler et al. (2014); Coachman et al. (1975); Grebmeier et al. (2015); Llinás et al. (2009); P. Stabeno (pers. comm.); Pickart et al. (2009); Pickart et al. (2013); Pickart and Corlett (2016); Pisareva et al. (2015); S. Danielson (pers. comm.); Sapozhnikov et al. (2011); Spall et al. (2008); Stabeno et al. (1999); Takahashi et al. (2011); University of Alaska Fairbanks Institute of Marine Science (2009); Walkusz et al. (2012); Weingartner (2006); Weingartner et al. (2005a); Weingartner et al. (2005b)

Neal Herbert / National Park Service

Ocean Currents

This map depicts typical surface current patterns with blue arrows, while deep circulation, which is less well understood, is shown with dashed lines. Freshwater inputs from major rivers are also shown, along with marine areas that are strongly influenced by terrestrial inputs of organic matter (as indicated by measurements of depleted ^{13}C in sediments).

Three water masses—the Alaska Coastal Current, the Bering Slope Current, and the Anadyr Current—flow north from the Bering Sea through the Bering Strait, carrying heat and nutrients north from the Pacific Ocean across the Chukchi shelf and into the Arctic Ocean. The low salinity, nutrient-rich waters of the Bering Sea help drive some of the world's highest marine productivity by bringing zooplankton and particulate organic carbon into the Bering Strait and the southern Chukchi Sea. Because of these circulation patterns, the Bering Strait is an important migratory corridor for birds and marine mammals.

Upwelling, the process by which bottom water is lifted to the surface, is also associated with high biological productivity. Areas with frequent upwelling events, such as the Bering Sea shelf break on the eastern Beaufort Sea near the community of Tuktoyaktuk, are often important feeding areas for bowhead whales and other marine mammals, as well as marine birds.

Sea Ice

Max Goldman and Erika Knight

Sea ice is a defining component of the Arctic. As habitat for many species, sea ice and the freezing waters in which it forms are integral to the persistence of the Arctic ecosystem. Sea-ice extent—the location of the ice margin—is a commonly used quantitative means of assessing changes in Arctic sea ice (Weeks 2010, Perovich et al. 2015). The ice margin reaches its southernmost maximum extent in March. Spring warming drives the margin northward over 1,000 miles (1,600 km) toward its September minimum extent (Gradinger 2008). Satellite-based passive microwave instruments (radar) have been used to map sea-ice extent and change since 1979 (Tschudi et al. 2015). Daily and monthly data on ice extent are available from the National Snow and Ice Data Center (NSIDC). The NSIDC satellite data show that freeze-up is arriving later by one to two weeks per decade for the Chukchi and Beaufort Seas and break-up is arriving earlier by a week or more every decade (Johnson and Eicken 2016)

Age is another important sea-ice metric. Older ice tends to be thicker and less susceptible to melting by solar radiation and warm currents than younger ice, or first-year ice. Age is determined using satellite observations and drifting buoy records that track ice over several years (Tschudi et al. 2010, Maslanik et al. 2011).

SETTING

Sea-ice margins are not only found at the extent of the ice, but they are also present throughout the pack ice in leads (large fractures in the ice) and polynyas (recurring areas of open water within the ice floe). Leads and polynyas are critical to many Arctic species. Leads are formed when wind or current-induced stress causes a crack to form in an expanse of ice. These cracks can range from a few feet to hundreds of feet wide. They are heavily utilized by seabirds and marine mammals, which rely on them to access forage resources beneath the ice, or as breathing holes while foraging (Divoky 1979, Perovich et al. 2013, Rode et al. 2014).

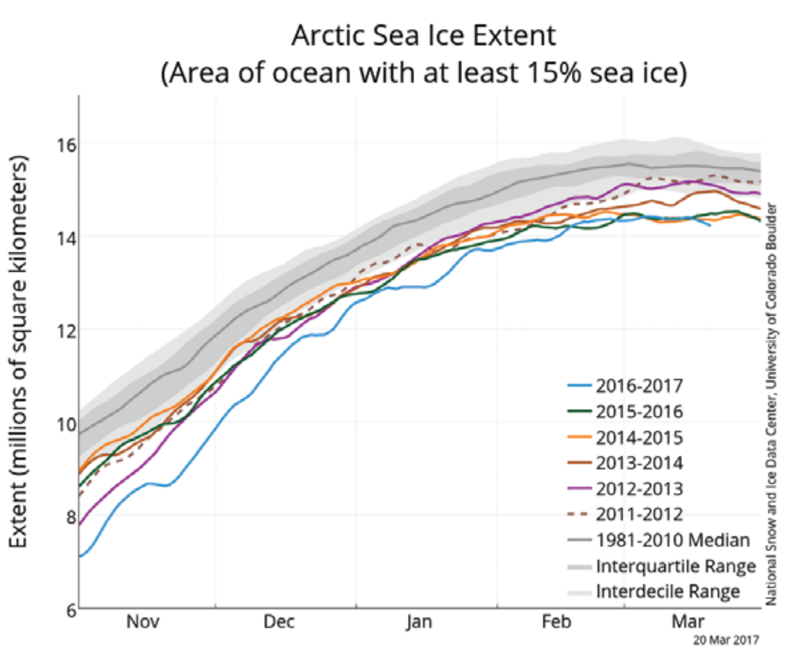

FIGURE 2.2-1. The graph above shows Arctic sea ice extent as of March 20, 2017, along with daily ice extent data for five previous years. The line for 2016 to 2017 is shown in blue, 2015 to 2016 in green, 2014 to 2015 in orange, 2013 to 2014 in brown, 2012 to 2013 in purple, and 2011 to 2012 in dashed brown. The 1981 to 2010 median is in dark gray. The gray areas around the median line show the interquartile and interdecile ranges of the data.

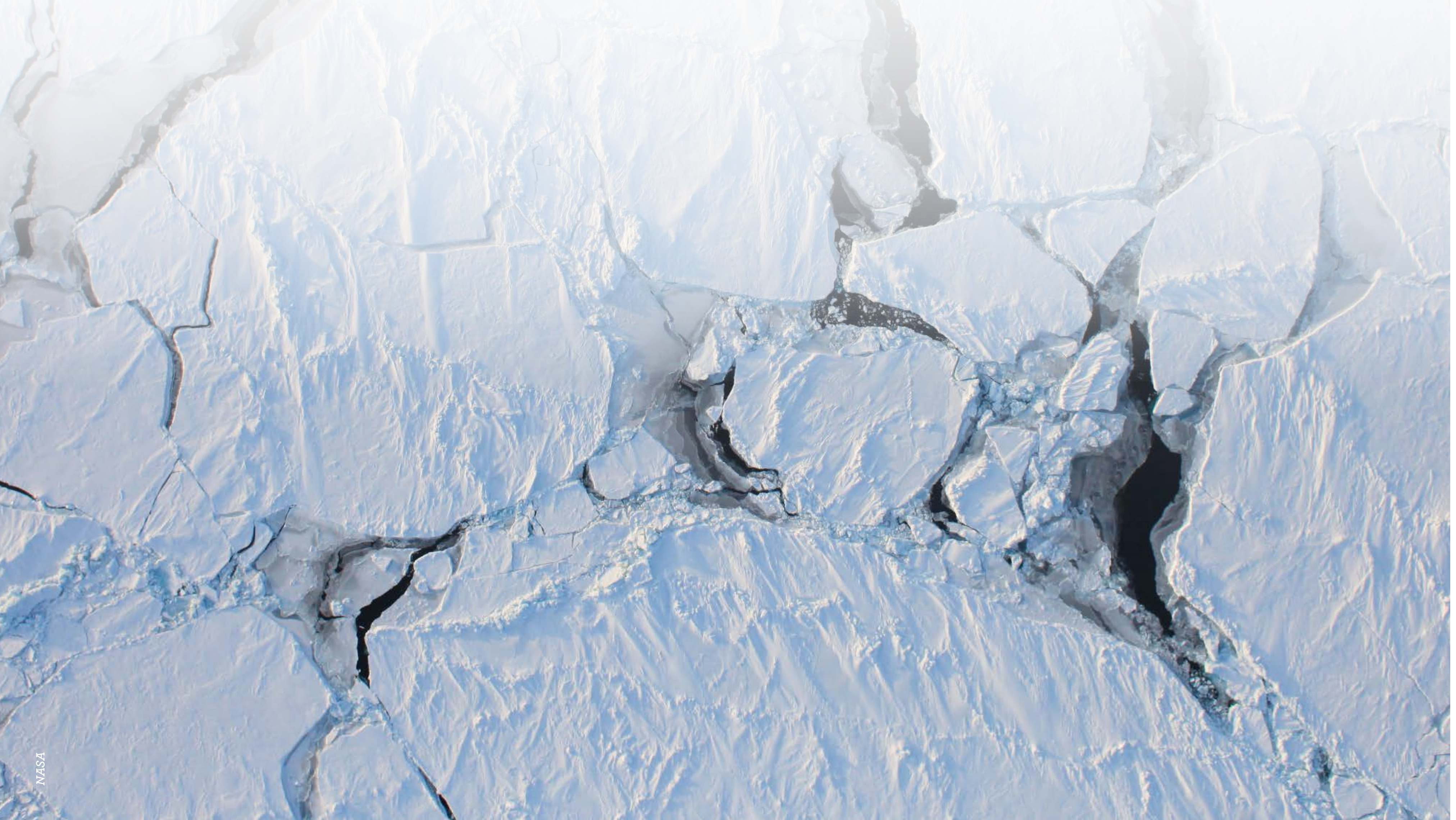

A polynya is an expanse of open water caused either by an upwelling of warm-water currents, by wind, or by a combination of these (Weeks 2010). Because polynyas are caused by perpetuating features, they tend to stay open much longer than leads, and often occur in the same places year after year, such as near St. Lawrence Island, Wrangel Island, Hanna Shoal, and the Yukon-Kuskokwim (Y-K) Delta. Polynyas are used by seabirds, waterfowl, seals, walrus (*Odobenus rosmarus divergens*), whales, and polar bears (*Ursus maritimus*) (Divoky 1979, Perovich et al. 2013, Rode et al. 2014).

ECOLOGICAL ROLE

The Bering-Chukchi-Beaufort Seas region is characterized by divergent sea-ice conditions (Amstrup et al. 2008). As temperatures cool in the fall, the sea-ice margin pushes south toward the Bering Strait. Land-fastened, or "fast" ice forms in early winter when surface winds and air temperatures freeze the relatively shallow waters near the coast. As fast ice merges with sea ice (pack ice), ice-obligate species, such as the polar bear, follow the south-moving ice edge where their prey species feed at the especially productive margins of ice and water (Rode et al. 2014). This productivity is due in large part to the available sunlight required to fuel photosynthesis in the water column, as well as the wind-shear-driven, strong currents near the ice edge, which drives upwelling, an important component to productivity. As the ocean surface freezes and ice accumulates, life in the Bering, Chukchi, and Beaufort Seas begins to concentrate at the sea-ice margins.

Sea ice in the Bering Sea is composed entirely of first-year ice (ice that formed in the current year, which is less than 3–6 feet [1–2 m thick]). As the weather warms in the spring, the southern ice extent recedes toward the northern Bering Sea. By late spring/early summer, fast ice begins to melt in the Bering Strait. The ice edge continues to move northward, and over the course of the summer, the ice pulls away (diverges) from the northeast Chukotka Peninsula, Wrangel Island, and northwest Alaska.

Ice in the Chukchi and Beaufort Seas is made up of first-year and multi-year ice about 5–10 feet (1.5–3 m) thick. By late summer, the ice diverges from the Canadian Beaufort Sea and little to no ice lingers atop the continental shelf in any of the three seas. Ice divergence from land affects ice-obligate species most intensely during late summer, as the ice margin recedes northward hundreds of miles from the coastline. These species then must either remain ashore and face potential conflicts with brown bears and humans, or follow the ice as it continues to retreat northward over deeper, less productive waters. In fall and winter, the process reverses as cold, dark days produce new ice that first expands into the southern Beaufort Sea, then the Chukchi Sea, and finally back through the Bering Strait into the Bering Sea.

CONSERVATION ISSUES

Sea ice is often used as a herald of global climate change. As air and sea-surface temperatures continue to warm, the annual sea-ice maximum and minimum extents in the Arctic continue to trend toward less coverage, with more open water and less multi-year ice (National Snow and Ice Data Center 2016). Even though the winter ice maximum reaches similar southern latitudes each year, the extent is not indicative of overall ice quality in the Arctic, which has continued to trend toward thinner and younger pack ice. These trends have resulted in an overall decrease in the quality of ice in the Arctic, as the core region of old, multi-year pack ice is thinning and melting each summer, and returning as first-year ice each winter.

Over the past decade, bottom melting in the Beaufort and Chukchi Seas has increased substantially. While ice-melt measurements dating back to 1959 indicate that more than half of the overall ice-melt happened on the surface, recent data show a shift in that paradigm. In the last ten years, bottom melting accounts for at least twice as much ice loss as surface melting, and is enough to remove much of the multi-year ice in the region. The greater amount of bottom melting in the Beaufort and Chukchi Seas is directly related to the solar heating of the upper ocean (Perovich and Richter-Menge 2015). Since ice and cold waters trap more carbon from the atmosphere than do warm waters, the Arctic Ocean is precariously positioned as the first to be impacted by changes in global temperature. This characteristic of sea ice, in turn, exacerbates the problem as even more sequestered carbon is released by the warming waters (Bouttes et al. 2010, Sigman et al. 2010, Sun and Matsumoto 2010, Parrenin et al. 2013, Abelmann et al. 2015).

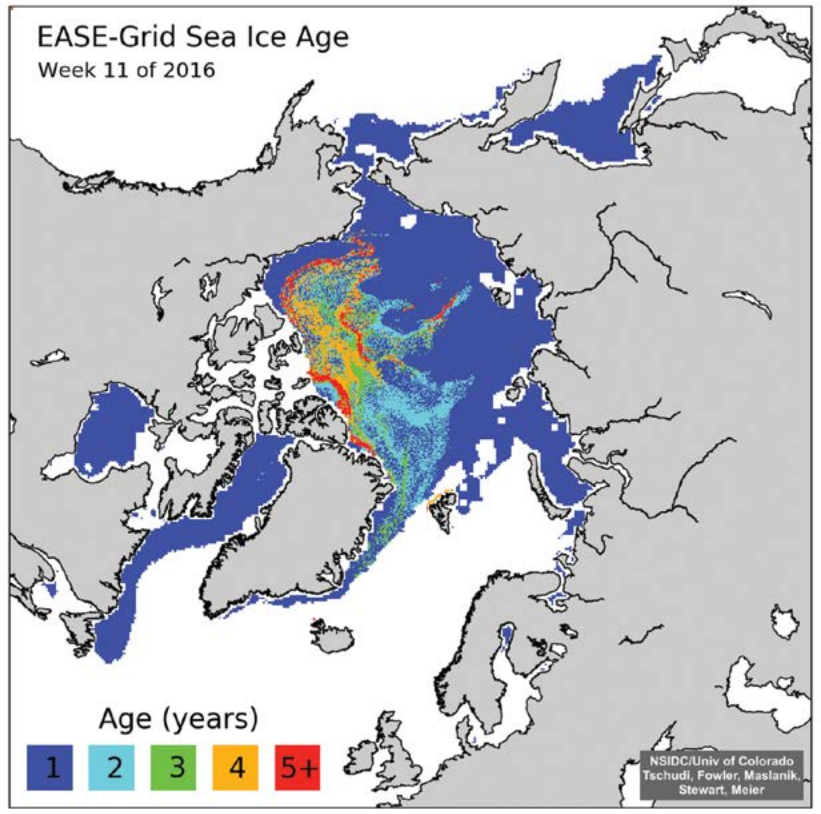

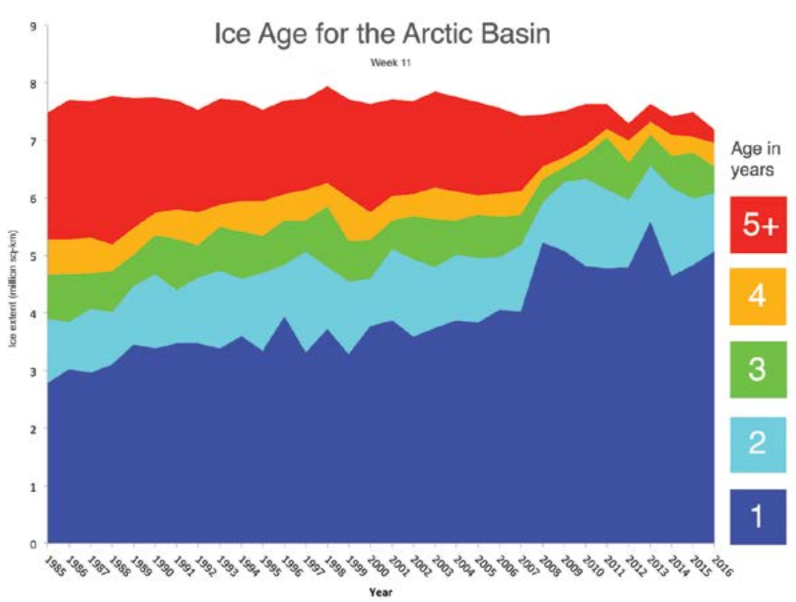

FIGURES 2.2-2 (TOP), 2.2-3 (BOTTOM). These figures show Arctic sea ice age from March 4 to 10, 2016. The top graph shows ice age distribution for that week alone and the bottom graph shows ice age distribution for that week from 1985 to 2016.

MAPPING METHODS (MAPS 2.2a–2.2.b)

Sea ice data are shown on two seasonal maps, one showing spring and summer sea ice retreat (March–September) and the other showing fall and winter sea ice advance (September–March). Each map shows monthly ice extent lines from two time periods: 2006–2015 and 1981–2010. In addition, historical March and September monthly ice extents from 1850 are shown. Areas where polynyas, recurring leads, or landfast ice occur are also shown.

Approximate median monthly sea-ice extent lines for 2006–2015 were analyzed by Audubon Alaska (2016c) using monthly sea-ice extent data downloaded from the NSIDC (Fetterer et al. 2016). For each month, the downloaded monthly ice-extent line shapefiles were merged across years (2006–2015) and converted to points, generating

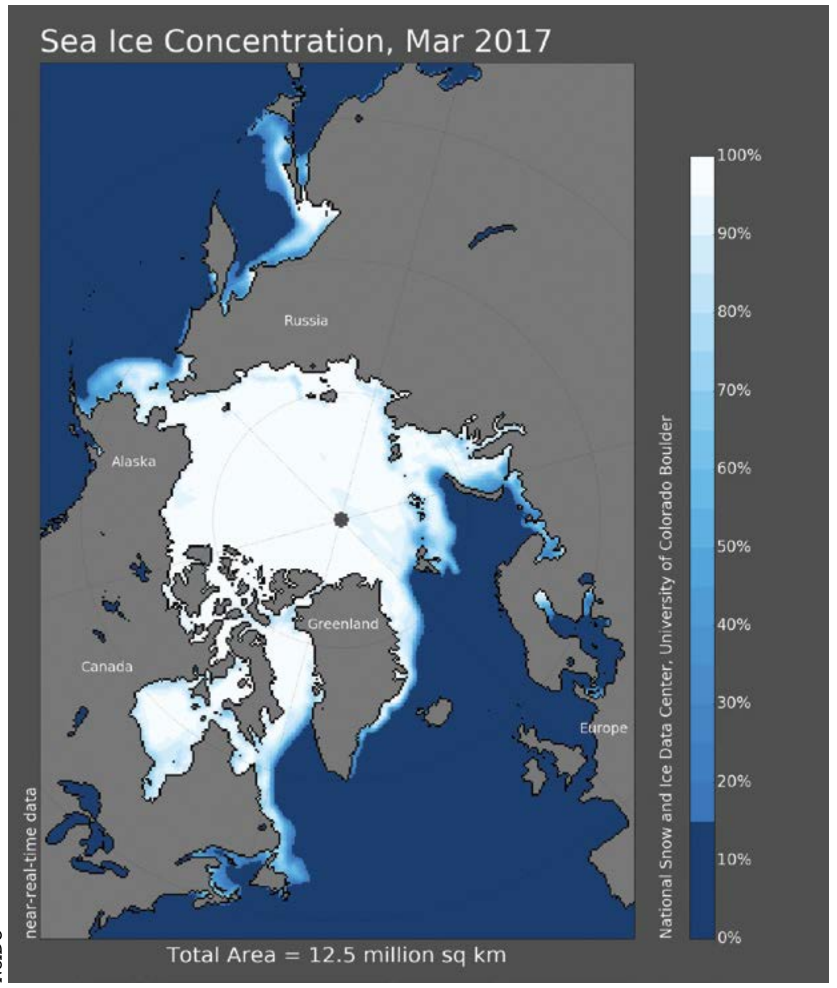

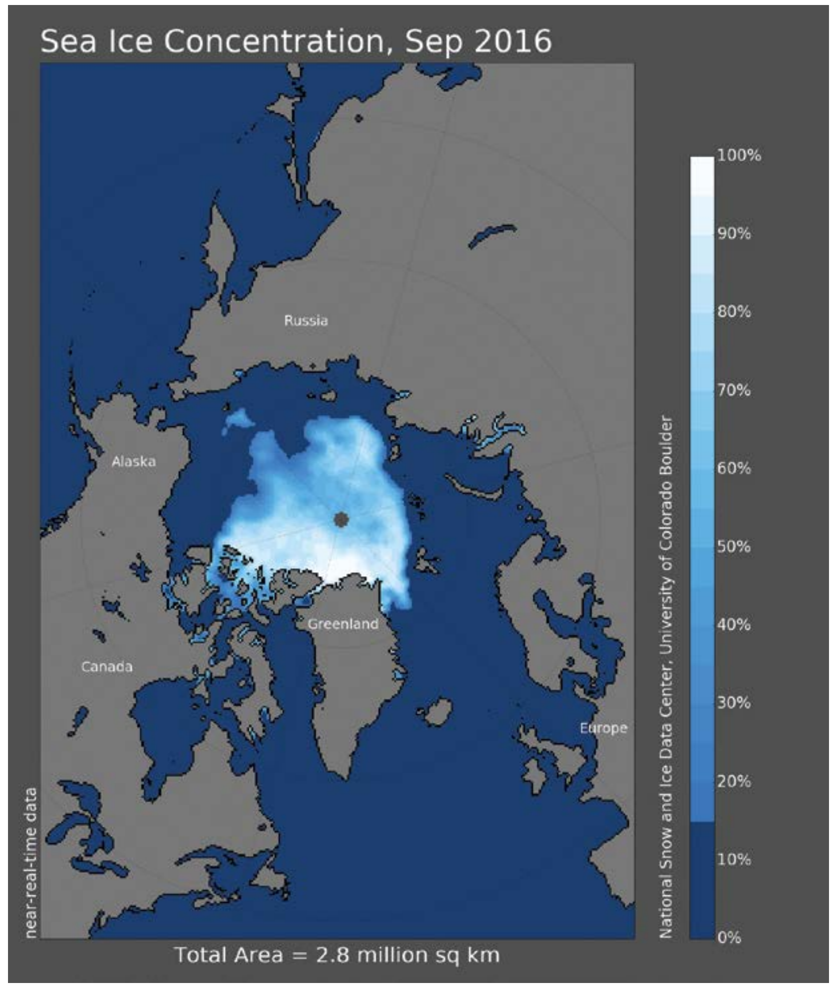

NSIDC

FIGURES 2.2-4 (LEFT), 2.2-5 (RIGHT). The monthly concentration images show a particular month's ice concentration with each 25-km data cell color-coded in shades of blue to white, where dark blue is 0% ice (ocean) and white is 100% ice. The area around the North Pole that is not imaged by the satellite is left out of the figures.

a point cloud for each month during this time period. Within each monthly point cloud, we found the midpoint of the northernmost and southernmost points along each 1-degree line of longitude across the project area; the midpoints were then connected and the resulting line smoothed.

The 1981–2010 median monthly sea-ice extent lines were downloaded from NSIDC (Fetterer et al. 2016). The southernmost winter ice-extent line was compiled from the Fetterer et al. (2016) 1980–2015 monthly ice-extent medians by Audubon Alaska (2016d). Historical ice extents from March and September 1850 were downloaded from Scenarios Network for Alaska and Arctic Planning (2016).

The polynyas and recurring leads data show the maximum areas in which polynyas and recurring leads are known to occur. The data come from several sources: Audubon Alaska et al. (2017), Carmack and MacDonald (2002), Oceana and Kawerak (2014), Stringer and Groves (1991), and an Audubon Alaska (2009) compilation of data from Eicken et al. (2005).

Landfast ice data were compiled by Audubon Alaska (2016b) based on landfast ice data available from Audubon Alaska et al. (2017), Carmack and MacDonald (2002), Eicken et al. (2009), National Oceanic and Atmospheric Administration (1988), National Snow and Ice Data Center et al. (2006), National Snow and Ice Data Center and Konig Beatty (2012), Oceana and Kawerak (2014), Satterthwaite-Phillips et al. (2016), and Spiridonov et al. (2011).

Data Quality
Sea-ice extent data are of high quality, based on remote sensing images covering the entire project area, at a spatial resolution of 15.5 miles (25 km). The extents encompass the area where the sea-ice concentration is measured at 15% or greater.

The polynya, recurring leads, and landfast ice data are of medium quality, compiled from several sources that have only partial coverage of the map area. Taken together, these data sources have good coverage of the map area with the exception of the Russian portion of the Bering Sea.

Reviewers
- Bering Strait Traditional Knowledge-Holder Map Review Workshop participants
- Mark Johnson

MAP DATA SOURCES

Approximate Monthly Sea-Ice Extent (2006–2015): Audubon Alaska (2016c) based on Fetterer et al. (2016)

Median Monthly Sea-Ice Extent (1981–2010): Fetterer et al. (2016)

Southernmost Winter Sea-Ice Extent (1980–2015): Audubon Alaska (2016d) based on Fetterer et al. (2016)

Historic (1850) March and September Ice Extents: Scenarios Network for Alaska and Arctic Planning (2016)

Polynyas and Recurring Leads: Audubon Alaska (2009) based on Eicken et al. (2005); Audubon Alaska et al. (2017); Carmack and MacDonald (2002); Oceana and Kawerak (2014); Stringer and Groves (1991)

Landfast Ice: Audubon Alaska (2016b) based on Carmack and MacDonald (2002), Eicken et al. (2009), National Oceanic and Atmospheric Administration (1988), and National Snow and Ice Data Center et al. (2006); Audubon Alaska et al. (2017); National Snow and Ice Data Center and Konig Beatty (2012); Oceana and Kawerak (2014); Satterthwaite-Phillips et al. (2016); Spiridonov et al. (2011)

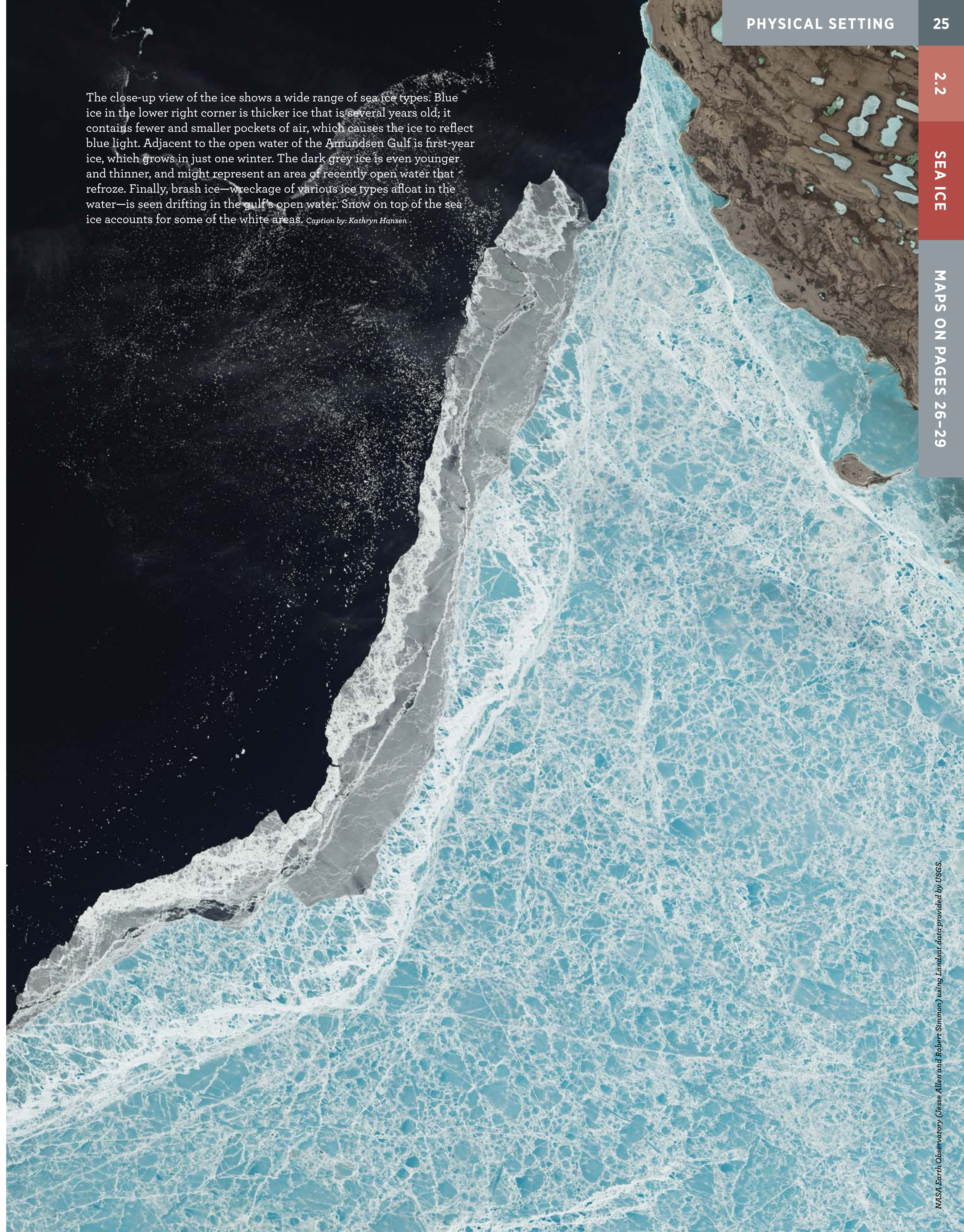

The close-up view of the ice shows a wide range of sea ice types. Blue ice in the lower right corner is thicker ice that is several years old; it contains fewer and smaller pockets of air, which causes the ice to reflect blue light. Adjacent to the open water of the Amundsen Gulf is first-year ice, which grows in just one winter. The dark grey ice is even younger and thinner, and might represent an area of recently open water that refroze. Finally, brash ice—wreckage of various ice types afloat in the water—is seen drifting in the gulf's open water. Snow on top of the sea ice accounts for some of the white areas. *Caption by: Kathryn Hansen*

NASA Earth Observatory (Jesse Allen and Robert Simmon) using Landsat data provided by USGS.

Sea Ice Advance

Map Authors: Erika Knight, Skye Cooley, Melanie Smith, and Max Goldman
Cartographer: Daniel P. Huffman

KAWERAK, INC.
Audubon ALASKA

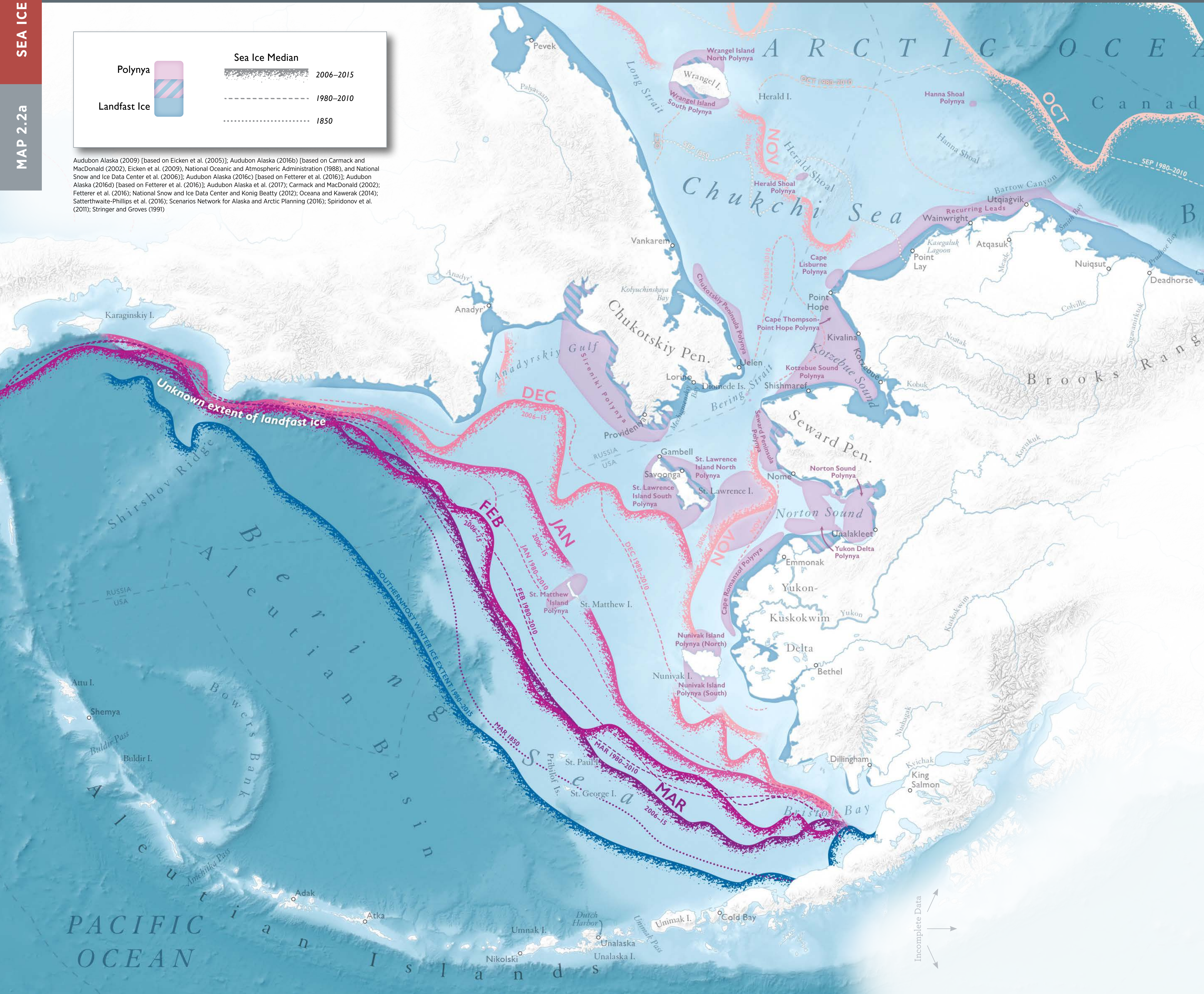

Audubon Alaska (2009) [based on Eicken et al. (2005)]; Audubon Alaska (2016b) [based on Carmack and MacDonald (2002), Eicken et al. (2009), National Oceanic and Atmospheric Administration (1988), and National Snow and Ice Data Center et al. (2006)]; Audubon Alaska (2016c) [based on Fetterer et al. (2016)]; Audubon Alaska (2016d) [based on Fetterer et al. (2016)]; Audubon Alaska et al. (2017); Carmack and MacDonald (2002); Fetterer et al. (2016); National Snow and Ice Data Center and Konig Beatty (2012); Oceana and Kawerak (2014); Satterthwaite-Phillips et al. (2016); Scenarios Network for Alaska and Arctic Planning (2016); Spiridonov et al. (2011); Stringer and Groves (1991)

National Park Service

Sea Ice Advance

As temperatures cool in the fall, the sea-ice margin advances south from the September minimum extent toward the Bering Strait. The sea-surface temperature drops as air temperature and photoperiod decrease, and ice begins to form in protected inlets and bays along the coastline. As the open ocean cools, needle-like ice crystals called frazil begin to turn the water into slush. As the temperature continues to drop and the ice floats to the surface, the frazil begins to accumulate and bond, eventually forming a solid sheet of ice. The ice crystals force the salt out into the water, resulting in sea ice consisting of mainly fresh water. As the ocean surface freezes and ice accumulates, life in the Bering, Chukchi, and Beaufort Seas begins to concentrate again at the sea-ice margin. Ice-obligate and ice-associated species follow the south-moving ice edge and seek out leads (large fractures in the ice caused by wind or pressure) and polynyas (recurring areas of open water formed by water currents and wind), as their prey species feed at the especially productive margin of ice and water.

Along the coastline in the Arctic, ice forms as water or drift ice freezes to the edge of the land. Land-fastened (fast) ice generally forms in early winter and unlike pack ice, is not impacted by the tides. Wind and currents dictate whether the pack ice will combine with the fast ice, and are responsible for the formation of polynyas. Leads can range from a few feet wide to hundreds of feet wide, and along with polynyas ensure that ice margins, and the life that relies on them, are present throughout winter. The ice margin continues to advance until late February or early March, when the maximum annual sea-ice extent is reached.

Sea Ice Retreat

Map Authors: Erika Knight, Skye Cooley, Melanie Smith, and Max Goldman
Cartographer: Daniel P. Huffman

KAWERAK, INC. Audubon ALASKA

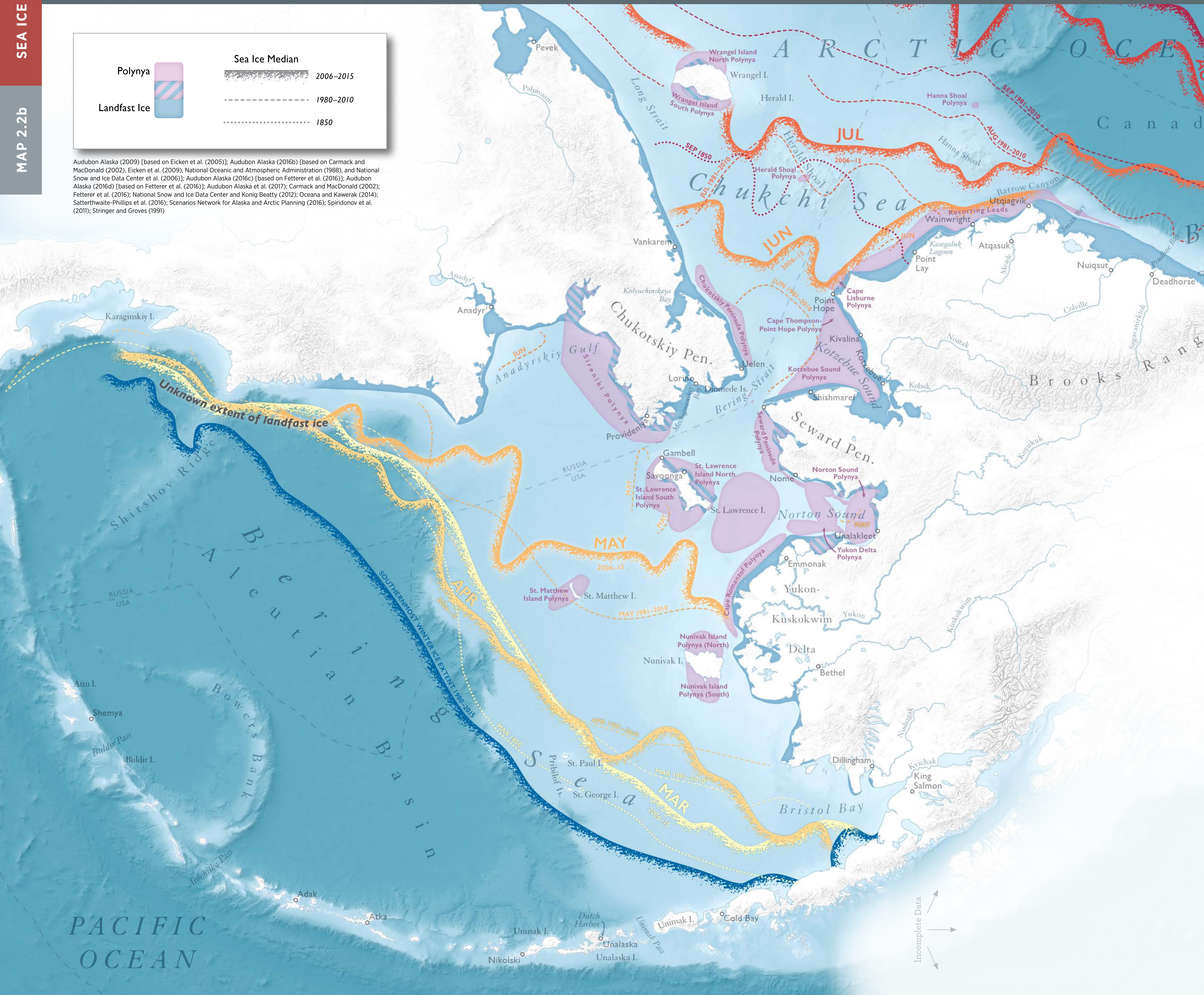

Audubon Alaska (2009) [based on Eicken et al. (2005)]; Audubon Alaska (2016b) [based on Carmack and MacDonald (2002), Eicken et al. (2009), National Oceanic and Atmospheric Administration (1988), and National Snow and Ice Data Center et al. (2006)]; Audubon Alaska (2016c) [based on Fetterer et al. (2016)]; Audubon Alaska (2016d) [based on Fetterer et al. (2016)]; Audubon Alaska et al. (2017); Carmack and MacDonald (2002); Fetterer et al. (2016); National Snow and Ice Data Center and Konig Beatty (2012); Oceana and Kawerak (2014); Satterthwaite-Phillips et al. (2016); Scenarios Network for Alaska and Arctic Planning (2016); Spiridonov et al. (2011); Stringer and Groves (1991)

Patrick Kelley / USCG

Sea Ice Retreat

The Bering, Chukchi, and Beaufort Seas host a dynamically changing ice margin. As the weather warms in the spring and summer, the ice pack recedes north from the maximum annual sea-ice extent in the Bering Sea that occurs each March. Pack ice first begins to melt as sunlight and air temperatures melt the surface, forming freshwater melt ponds atop the ice until it breaks, and the melted fresh water and salty seawater mix. Later, when seawater temperatures have also increased, sea ice will begin to melt from the bottom and top simultaneously, causing the margin to recede more quickly.

After the pack ice has begun to break up and recede, fast ice begins to melt. It melts first along the coasts of Russia and Alaska in the Bering Sea, then through the Bering Strait, then along the northeast Chukotka Peninsula, Wrangel Island, and northwest Alaska, and finally through the Beaufort Sea until the ice margin has fully pulled away from the Arctic coastline in September. As the ice quality degrades, the pack ice and ice floes break up due to rough seas and collision, increasing the surface area exposed to warming air temperature. The degradation of the ice allows sunlight to penetrate to the water column and primary productivity begins with blooms of photosynthetic life. This surge of life ripples throughout the food web, all the way to the apex predators that follow their prey, and to the ice margins, as they all move farther and farther north. Each decade the minimum ice extent recedes farther north due to global climate change, beyond Alaska's continental shelf. Benthic feeders are forced to choose to either follow the ice off of the continental shelf and risk starvation, or come ashore and face other risks.

Climate

Melanie Smith

The Bering, Chukchi, and Beaufort Seas are considered Arctic seas based on physical climate characteristics. Starting with seawater temperature and sea ice, the physical climate is a determining factor in the ecology and distribution of organisms that inhabit marine waters.

The southernmost of the three seas, the Bering Sea is technically the northernmost sea of the Pacific Ocean, but ecologically it acts like an Arctic sea. For purposes of policy and decision-making, the Bering Sea is an Arctic sea as well. Although multiple definitions of the Arctic exist (e.g. Arctic Circle, Arctic Ocean), the US Arctic Research and Policy Act of 1984 (ARPA) defines the Arctic as “including the Arctic Ocean and the Beaufort, Bering and Chukchi Seas; and the Aleutian chain.”

SETTING

The Bering Sea is north of the Gulf of Alaska and south of the Arctic Ocean, separated from the rest of the North Pacific by the Aleutian Island chain. The US (Alaska) lies to the east and Russia lies to the west. The Bering Sea covers 590 million acres (2.4 million sq km). For comparison, the landmass of Alaska is 425 million acres (1.7 million sq km). In the eastern Bering Sea (EBS), the continental shelf extends 300–450 miles (480–725 km) west from the Alaska mainland. Around a depth of 650 feet (200 m), the shelf breaks abruptly to much greater depths, to below 10,000 feet (3,050 m) in the Aleutian Basin. These deep waters characterize the western Bering Sea. The volcanic chain of the Aleutian Islands rises sharply from the seafloor below. At the subducting edge of the Pacific Plate, these undersea mountains emerge at the edge of the Aleutian Trench. At nearly 5 miles (8 km) deep, the Trench is one of the deepest parts of the world’s oceans.

At the north end of the Bering Sea, the Bering Strait is a 53-mile-wide (85-km) passage, which is the only marine connection between the Pacific and Arctic Oceans. All of the physical properties and marine life exchanged between the two oceans are facilitated by and through the Strait. To the north of the Bering Strait lies the Chukchi Sea. This shallow Arctic sea spans waters from Point Barrow, Alaska, to Wrangel Island, Chukotka (Russia). Two prominent shoals, Hanna and Herald, influence ice patterns and water mass movement. The Chukchi Sea covers 153 million acres (240,000 sq km).

At the seam between the Chukchi and Beaufort Seas, Barrow Canyon cuts a deep trough through the continental shelf, creating an area of mixing and upwelling of significant productivity. The Beaufort Sea stretches from Point Barrow east to the Amundsen Gulf in Canada. In the Beaufort, the continental shelf stretches only about 60 miles (100 km) offshore before descending steeply into the Canada Basin, reaching 12,500 feet (3,800 m) deep, or about 2.4 miles (3.8 km). The Beaufort Sea covers 45 million acres (184,000 sq km).

ECOLOGICAL ROLE

Based on an analysis of associations of zooplankton, fishes, and birds, Sigler et al. (2011) described three major biogeographic provinces in the Alaska marine domain that loosely align with the geographic boundaries of these seas, but with some important differences.

- The Eastern Bering Shelf Province covers the continental shelf waters of the central and southern Bering Sea, a predominantly subarctic pelagic system not as dominated by sea ice as areas farther north. This is a region of very high productivity for both pelagic and demersal fishes, which are limited in their northern distribution by the “cold pool” that forms from annual ice melt.

- The Chirikov-Chukchi Province includes Bering Sea waters north of St. Lawrence Island and waters of the Chukchi Sea. This is a shallow, benthic-dominated, ice-driven system heavily influenced by nutrients and productivity carried north from the Bering Sea (Grebmeier et al. 2006). This region has some of the highest water-column production (Springer and McRoy 1993) and benthic infaunal biomass (fauna that lives within the ocean floor) in the world (Grebmeier et al. 2006).

- The third province, the Beaufort Sea, is a narrow shelf area with ecological patterns driven by winds, upwellings, and river inputs. This region is largely isolated from the influence of the Bering Sea, instead receiving inputs from the Canada Basin and Amundsen Gulf regions. Although this region has lower overall productivity, benthic-pelagic coupling is strong, providing ample food resources for bottom feeders, including a high abundance of sea ducks.

The Marine Ecoregions of Alaska (Piatt and Springer 2007) further divide these biogeographic provinces into more than 20 subregions of ecological similarity. These subdivisions are useful for characterizing the physical and biological setting of this region at a finer scale, and for comparison among subregions.

Change

Using data from the National Oceanic and Atmospheric Administration (NOAA) Pacific Marine Environmental Laboratory (PMEL) (Hermann et al. 2013), Smith and Koeppen (2016) analyzed data representing recent and future predicted conditions across the Bering Sea (not available for the Chukchi and Beaufort Seas). Data for recent conditions are annual averages from a hindcast model covering 1965–2009, and data for future conditions represent the projected average total change from 2003–2040. These model results will be referred to throughout this summary. Read the Mapping Methods section for details on the models and methods used.

Seawater Temperature (Maps 2.3a–2.3d)
Seawater temperature is influenced by depth, ocean currents, and sea ice, as well as tides and surface winds that move and mix the water column. Deeper water tends to be cooler than shallow water at the same location. A defining feature is the cold pool, which forms over the EBS shelf as a consequence of melting sea ice. Commonly defined as the 35.6° F (2° C) isotherm, the cold pool has shifted northward over the last 3 decades by approximately 143 miles (230 km) (Mueter and Litzow 2008). This feature determines the distribution of Arctic and subarctic fishes and invertebrates, and its migration has caused a shift in species’ ranges. Further projected warming in the EBS of up to +3.1° F (+1.7° C) by 2040 (Hermann et al. 2013, Smith and Koeppen 2016) will likely continue the trend of northward movement of some Arctic, cold-adapted organisms, with replacement by other subarctic, warmer-water organisms, although species-specific responses are hard to predict (Mueter and Litzow 2008).

Based on the average annual temperature in the top 200 feet (60 m) of the water column, the warmest waters in the Bering Sea are in the Central Aleutians at 42.8° F (6.0° C), as well as the Aleutian Arc (41.4° F [5.2° C]) and Western Aleutians ecoregions (40.6° F [4.8° C]). The coolest waters are in the Anadyr Stream at just above freezing (32.5° F [0.3° C]). These shallow waters are expected to increase in temperature across the entire Bering Sea, with the exception of the Western Aleutians, which indicate a cooling of -0.2° F (-0.1° C). The greatest warming is predicted for the Bering Sea Shelf Edge ecoregion, also known as the Green Belt, and the neighboring EBS Outer Domain, with temperatures rising by +2.3° F (+1.3° C).

In deeper waters, 250–650 feet (75–200 m), overall temperatures are 0.7° to 2.0° F (0.4° to 1.1° C) cooler than shallow waters within the same ecoregion. Similar to the shallow waters, the Eastern Aleutians (42.1° F [5.6° C]), Central Aleutians (41.5° F [5.3° C]), and Aleutian Arc (39.4° F [4.1° C]) are the warmest ecoregions in the Bering Sea. The coolest ecoregion is again the Anadyr Stream, which is below

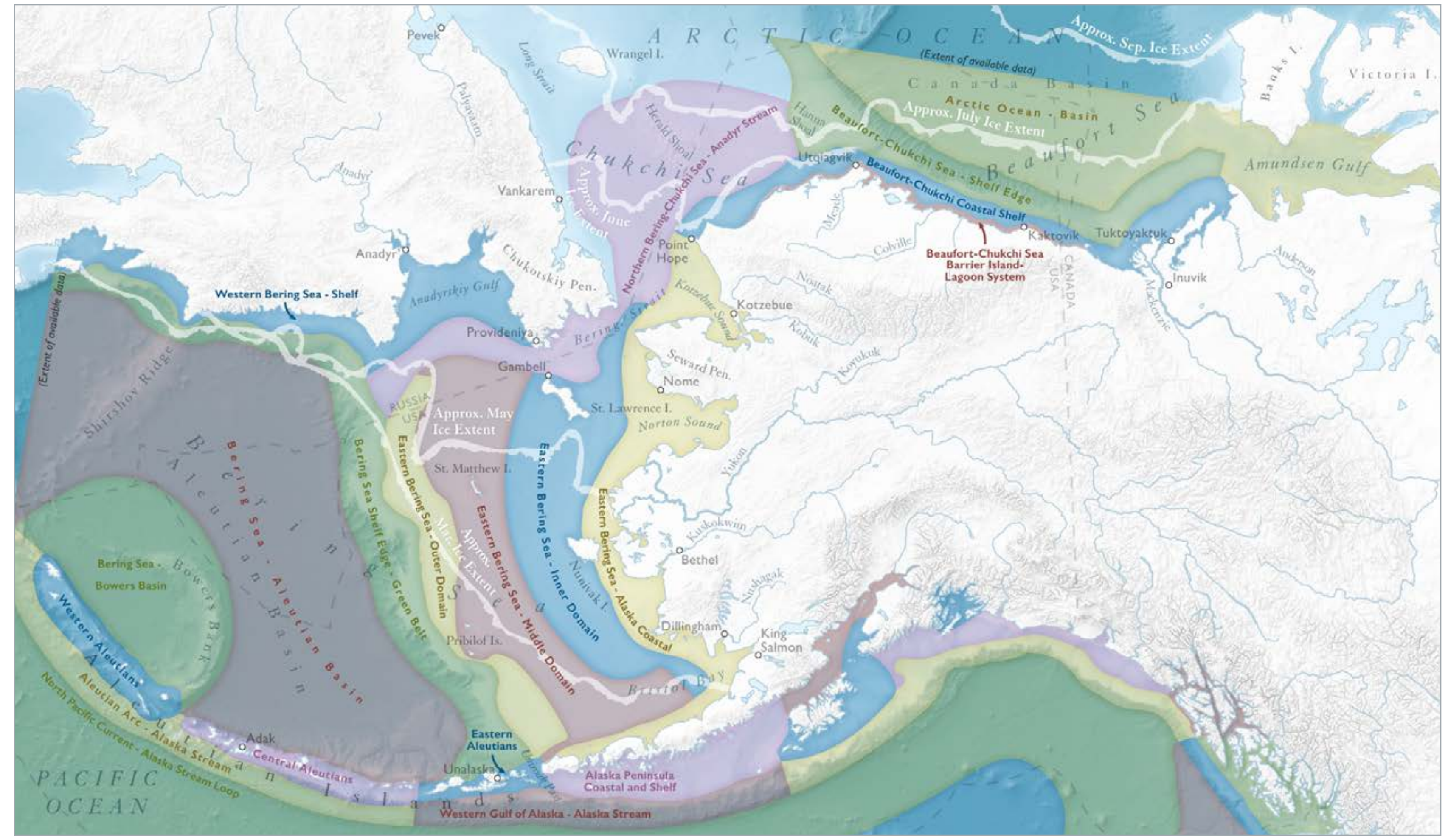

FIGURE 2.3-1. The Marine Ecoregions of Alaska (Piatt and Springer 2007) divide the Bering, Chukchi, and Beaufort Seas into more than 20 biogeographic provinces of ecological similarity. These subdivisions are useful for summarizing the physical and biological setting of smaller regions, and for characterizing differences between regions.

freezing on an annual basis, at 31.8° F (-0.1° C). In the future, the Western Aleutians and Aleutian Arc ecoregions may cool slightly, by -0.4° F (-0.2° C). However, the deep waters as a whole will experience considerable warming of up to +2.2° F (+1.2° C) along the Green Belt, and +1.8° F (+1.0° C) in the neighboring EBS Outer Domain.

Sea Ice (Maps 2.3e–2.3f)
Sea ice is a driving factor in the distribution of wildlife in the Bering, Chukchi, and Beaufort Seas. Sea ice can be a welcome platform for resting (e.g. Pacific walrus [*Odobenus rosmarus divergens*]) or an impediment to reaching foraging areas beneath (e.g. ringed seals [*Pusa hispida*]). Most activity occurs at the ice edge. Sea ice is in significant decline in concentration, extent, thickness, and timing of coverage (Meier et al. 2014). Experts predict an ice-free Arctic Ocean sometime this century (Wang and Overland 2009, Wang and Overland 2015). The timing of sea ice is changing, such that ice is arriving later and departing earlier. Declines have occurred in all months, with the smallest declines in winter and the largest declines in summer (Meier et al. 2014). Bering Sea ice is first-year ice that is pushed south from higher latitudes by winds, translating into less change to the sea-ice maximum extent that occurs each March. Arctic seas have historically been covered in multi-year pack ice, which is today greatly diminished, resulting in the greatest change in the sea-ice minimum extent each September.

In the Bering Sea, sea ice is most concentrated in the Anadyr Stream ecoregion (42% annual average concentration across the ecoregion), followed by the EBS Inner Domain (36%) and the Western Bering Sea Shelf ecoregion (35%). The Aleutian Basin, Aleutian Islands, and Gulf of Alaska are ice-free all year. Predicted changes in sea ice indicate loss across all ecoregions. The EBS Middle Domain ice concentration will decline the most (-9%), followed by the neighboring EBS Inner Domain to the east (-8%), and the Western Bering Sea Shelf (-7%) along the Russian coast. Overall, the combined Bering Sea continental shelf ecoregions will see an average of -7% sea-ice concentration as an annual average.

Phytoplankton (Maps 2.3g–2.3h)
When sea ice melts, it leaves behind nutrients in the form of ice algae, and kickstarts primary production in newly open waters (Horner and Schrader 1982). These two sources of phytoplankton are the basis of the food chain that fuels the Arctic ecosystem, feeding zooplankton that in turn feed fishes, marine birds, and marine mammals (Divoky 1979, Bradstreet and Cross 1982). Due to short food chains and tight pelagic-benthic coupling in these Arctic waters, changing sea-ice extent and timing can rapidly ripple throughout the marine ecosystem from primary production to higher trophic levels and is a major concern surrounding a changing climate (Grebmeier et al. 2006, Moline et al. 2008).

Specific to ice algae in the Bering Sea, average ecoregional productivity is highest in the Anadyr Stream, at 31 mg C / m^3. This area is followed by the EBS Outer Domain (29 mg C / m^3) and the neighboring EBS Middle Domain (25 mg C / m^3). Looking forward to 2040, ice phytoplankton will, as a spatial average, decrease for all ecoregions. The greatest loss of productivity is expected for the EBS Outer Domain (-20 mg C / m^3), which will lose two-thirds of its phytoplankton biomass. The Green Belt will be also highly affected, losing virtually all of the ice phytoplankton productivity received in the past (-16 mg C / m^3).

Microzooplankton (Maps 2.3i–2.3j)
Microzooplankton are a group of planktonic grazers ranging from 0.0008–0.008 inches (20–200 μm) in size. This group includes both single-celled (protist) and multi-celled (metazoan) organisms such as dinoflagellates, ciliates, radiolarians, foraminiferans, rotiferans, and mesoplanktonic larvae, among others (Calbet 2008). Microzooplankton are an important yet understudied link in the food chain as primary grazers of phytoplankton, which are consumed by larger meso-zooplankton. Microzooplankton graze heavily on phytoplankton, consuming on average 57% of the primary production per day in the Arctic (Schmoker et al. 2013).

In the Bering Sea, microzooplankton production in the top 200 feet (60 m) of the water column is highest in Unimak Pass and the surrounding Eastern Aleutians ecoregion (10.0 mg C / m^3), and along the Bering Sea Shelf Edge Green Belt (9.2 mg C / m^3) and the neighboring EBS Outer Domain (9.0 mg C / m^3). Future production is predicted to stay the same or somewhat decrease in these areas of recent highest productivity (0 to -0.2 mg C / m^3), while the Western Aleutians (+1.7 mg C / m^3; +23%) and Aleutian Arc ecoregions (+1.5 mg C / m^3; +26%) are expected to see the largest increases in microzooplankton production.

Copepods (Maps 2.3k–2.3L)
Copepods are a type of aquatic mesozooplankton—small crustaceans commonly <0.1 to 0.3 inches (1 to 8 mm) in size. Calanoid copepods are large, energy-rich copepods of the genera *Neocalanus* and *Calanus*, which dominate open waters of the North Pacific. Copepods are adapted to capitalize on the intense primary productivity in the water column associated with the moving sea-ice edge (Conover 1988). They are an important link in the food chain, grazing on phytoplankton and (to a lesser extent) other zooplankton, and providing a major food source for fishes, birds, and whales. Some upper-trophic species, like North Pacific right whales (*Eubalaena japonica*) and Least Auklets (*Aethia pusilla*), feed almost exclusively on *Neocalanus* in the Bering Sea (National Oceanic and Atmospheric Administration 2006, Bond et al. 2013).

On average, the EBS Alaska Coastal ecoregion has the highest biomass of large copepods in the upper 200 feet (60 m) of the Bering Sea (1.0 mg C / m^3). The neighboring EBS Inner Domain is next in copepod biomass (0.5 mg C / m^3), followed by the Eastern Aleutians ecoregion (0.5 mg C / m3). Copepod biomass is expected to decline slightly in the Eastern Aleutians (< -0.1 mg C / m^3) with other areas maintaining similar levels of productivity or seeing an increase. The greatest increase (< +0.1 mg C / m^3) will be in the Aleutian Arc. Overall, copepod productivity appears relatively stable across space and time.

Euphausiids (Maps 2.3m–2.3n)
Euphausiids are small, shrimp-like crustaceans, also known as krill (*Thysanoessa* spp.), about 0.8–1.0 inch (20–25 mm) in size. Like copepods, they feed on phytoplankton and, to a lesser extent, other zooplankton, and provide a highly important food source for upper trophic species. Euphausiids are the main prey of baleen whales, as well as many species of marine birds and fishes.

The Green Belt is the top area for euphausiid production, averaging 3.1 mg C / m^3 throughout waters to 200 feet (60 m) depth. Similar in productivity to the Green Belt is the Eastern Aleutians ecoregion, including Unimak Pass (3.1 mg C / m^3). Both areas are well known for the incredibly high densities of foraging seabirds such as shearwaters (*Puffinus* spp.) as well as fin (*Balaenoptera physalus*), gray (*Eschrichtius robustus*), and North Pacific right whales. The lesser-studied Western Bering Sea Shelf ecoregion also shares densities on par with these areas (2.9 mg C / m^3). The Green Belt is predicted to see the greatest loss in euphausiid productivity (-0.20 mg C / m^3; -6%), followed by the neighboring EBS Outer Domain (-0.12 mg C / m^3; -4%). The greatest increase in euphausiid productivity will be in the Aleutian Arc (+0.44 mg C / m^3; +23%) and Western Aleutians ecoregions (+0.43 mg C / m^3; +17%).

Benthic Infauna (Maps 2.3o–2.3p)
These Arctic seas, especially from St. Lawrence Island and north, are highly productive benthic ecosystems founded on the massive amounts of primary productivity at the migrating sea-ice edge. Including ice algae and water column blooms, more phytoplankton are produced than are utilized by water-column grazers (micro- and mesozooplankton). This unexploited nutrient source instead falls to the bottom of the sea, fertilizing an abundance of benthic organisms (Grebmeier et al. 2006). As a result, the northern Bering and Chukchi Seas have some of the highest benthic biomasses in the world (Grebmeier et al. 2006). The Chukchi Sea benthic infaunal assemblage is dominated by polychaetes, mollusks, and crustaceans, providing important food sources for Pacific walrus, gray whales, and eiders (Schonberg et al. 2014).

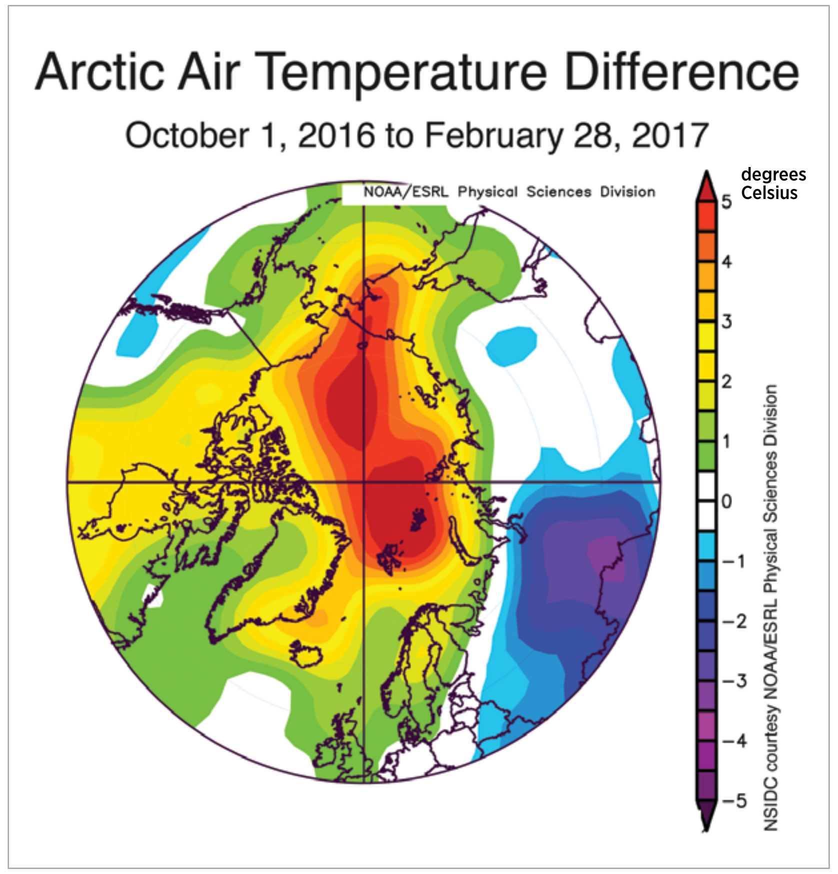

FIGURE 2.3-2. The plot shows Arctic air temperature differences at the 925 hPa level (about 2,500 feet [760 m] above sea level) in degrees Celsius from October 1, 2016 to February 28, 2017. Yellows and reds indicate temperatures higher than the 1981 to 2010 average; blues and purples indicate temperatures lower than the 1981 to 2010 average.

In the Bering Sea, benthic infaunal biomass is highest, on average, across the Western Bering Sea Shelf ecoregion (4542 mg C / m^2), followed by the EBS Alaska Coastal region (4085 mg C / m^2), and the EBS Middle Domain (4028 mg C / m^2). Modeled future values indicate that benthic biomass will be redistributed across the region, with both large gains and losses expected. In the Bering Sea, the greatest negative change in benthic infaunal biomass is predicted for the EBS Alaska Coastal ecoregion (-359 mg C / m^2) and the EBS Outer Domain (-175 mg C / m^2); the greatest increase is expected in the Anadyr Stream (+371 mg C / m^2) and Western Bering Sea Shelf (+293 mg C / m^2), already among the most productive areas. The Aleutian Islands and deeper off-shelf areas are expected to hold steady.

CONSERVATION ISSUES

Climate is a fundamental determining factor in the ecology and natural history of species. Conservation issues related to climate are a function of anticipated changes from a warming planet. The Arctic is warming at twice the rate of the global average. Experts predict that climate change will have major effects on physical, ecological, social, and economic systems around the world over the next century.

Physical changes include melting permafrost, sea ice, and glaciers; loss of ice on the surface reduces the planet's reflectance (albedo), causing additional warming than by atmospheric forcing alone. Melting also freshens ocean waters and changes salinity. Melting glacial ice causes sea levels to rise, while melting sea ice opens vast stretches of ocean, allowing greater storm surges to occur. Sea-level rise, storm surges, permafrost thaw and slumping, and stronger storms cause coastal erosion and inundation of low-lying areas or villages (Arctic Climate Impact Assessment 2004).

Social and economic impacts of climate change are both positive and negative, depending on the perspective. Increased flooding will cost communities and force them to relocate at very high expense, bringing great cultural losses associated with moving from a place of long-standing traditional use. Food security may be compromised due to

FIGURE 2.3-3. Every spring, the expansive pack of sea ice that covers the Beaufort Sea during the winter starts to thin and break up when the spring sunlight arrives and temperatures rise. Normally, that breakup does not reach full swing until late May. In 2016, unusually warm temperatures during the first few months of the year set the stage for early breakup. In April, a high-pressure system producing strong southeasterly winds parked itself over the Beaufort Sea and sent chunks of ice swirling in a clockwise direction in the Beaufort Gyre. The lower images show different stages of the ice breakup in April 2016. For comparison, the upper two strips show what conditions were like in April 2014 and April 2015. Notice how much more open water appears in 2016 than in the other years.

changing conditions (timing of ice, shore ice too weak for hunting, and stronger storms), as well as shifting of wildlife ranges (Marine Mammal Commission 2000). There may be an increase in vessel traffic in Arctic waterways and greater access to natural resources, bringing new ports, roads, pipelines, and jobs. Fisheries may be enhanced (Arctic Climate Impact Assessment 2004). Native communities are facing challenges to their traditional ways of life, and stand to bear the most immediate and acute effects from a changing climate. Native people should be consulted and included in ecological studies and policy decisions affecting the natural resources in their respective regions (Marine Mammal Commission 2000, Moller et al. 2004, Martello 2008, Laidre et al. 2015).

Ecological impacts will be widespread, and while some are already occurring or reasonably foreseeable, many others will be difficult or impossible to predict. The timing of spring primary production is regulated by climate conditions that control the timing of sea-ice retreat. This, in turn, has a major effect on ecological relationships at the base of the food chain. Under cool conditions, sea ice is more extensive and thicker, and melts later in the spring (late March or later). The nutrients released by the ice in the form of under-ice algae disperse at a time when there is ample daylight to warm the water and fuel a massive ice-edge phytoplankton bloom (April–May). Under these conditions, cooler water inhibits the production of zooplankton and recruitment of fish, and consequently the grazing of phytoplankton; more of the productivity sinks to the benthos. Under warm conditions, ice melts earlier (mid-March or before), when there is not enough daylight to support a bloom, and instead the bloom happens later in the summer (May–June), when water column conditions are right. Under these conditions, zooplankton and fishes thrive and more of the productivity flows into the pelagic food chain (Hunt et al. 2002, Hermann et al. 2013). The reorganization from a benthic-driven to pelagic-driven food web in sea-ice regions is a major shift in the ecology of Arctic seas, and the vulnerability of the ecosystem is thought to be high. With short food chains, changes in lower trophic levels can rapidly impact higher trophic levels, especially for benthic-feeding seabirds and marine mammals (Grebmeier et al. 2006).

Warming water temperatures can have unanticipated consequences, such as with walleye pollock (*Gadus chalcogrammus*) productivity (Sigler et al. 2011). This Subarctic species was expected to increase in abundance in warmer waters, but instead, warmer years led to a large decrease in pollock productivity, while cooler years led to an increase. In warm years, the ice-associated spring bloom led to a major decline

2.3 CLIMATE MAPS ON PAGES 36–37

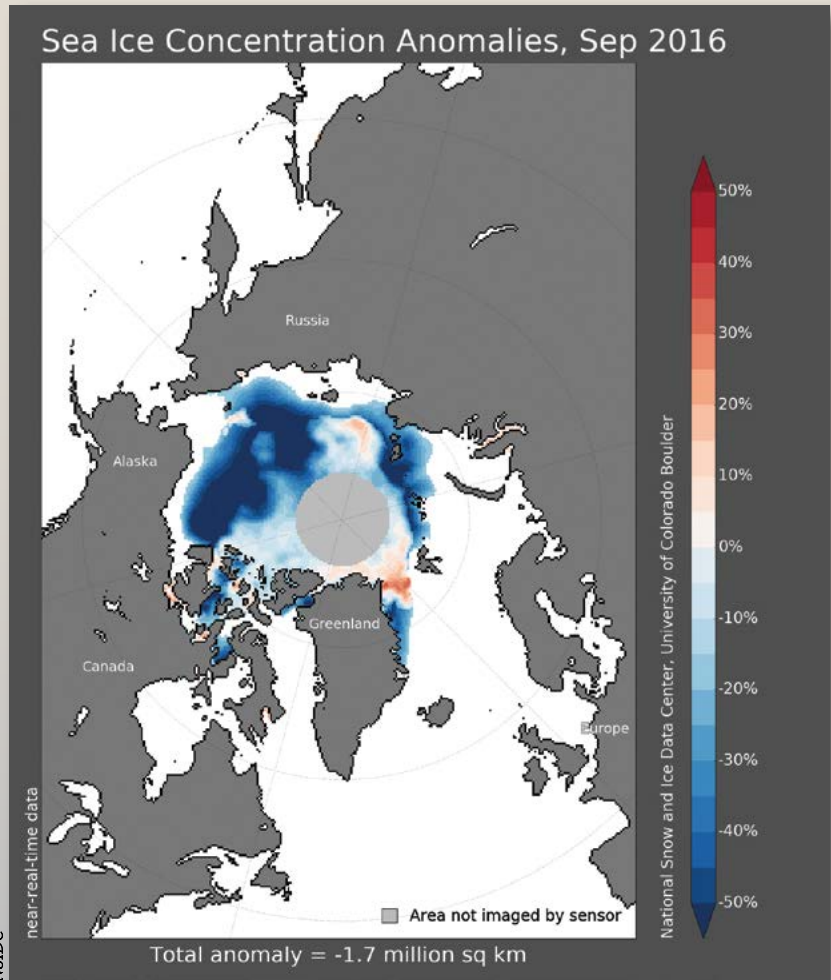

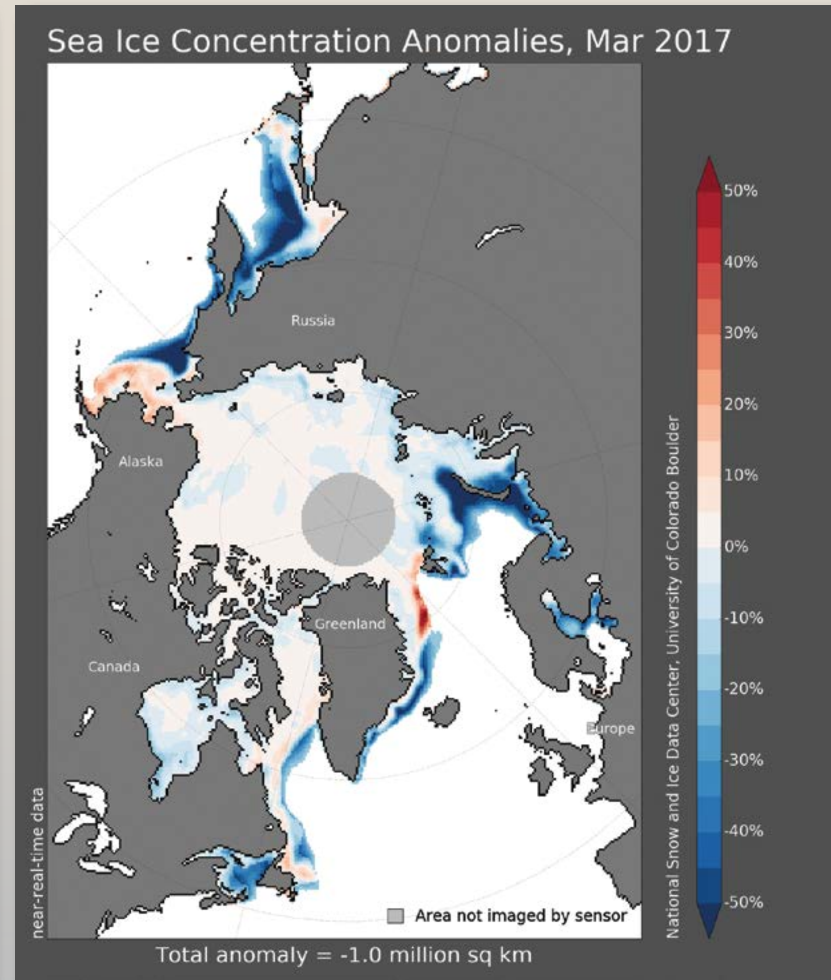

NSIDC

FIGURES 2.3-4 (LEFT), 2.3-5 (RIGHT). These images of anomalies in ice concentration show, in percent color-coded in shades of blue (negative anomaly) to red (positive anomaly), how much the ice concentration for a month differs from the mean calculated for that month over the 1981 through 2010 time range. The total anomalous area of sea ice for that month is also shown in the bottom margin of the image. The area around the North Pole that is not imaged by the satellite is left out of the images.

Melanie Smith / USFWS

Sunrise from the Chukchi Sea just offshore of Point Hope.

2.3 CLIMATE MAPS ON PAGES 36–37

in copepod and euphausiid abundance—key forage for juvenile pollock. Additionally, other larger fish accustomed to foraging on zooplankton took to foraging more intensely on juvenile pollock.

Species ranges are already shifting in response to climate changes. Mueter and Litzow (2008) found that the center of distribution for the 40 taxa they studied moved northward an average of 21 miles (34 km), including Arctic cod (*Arctogadus glacialis*), walleye pollock, Pacific halibut (*Hippoglossus stenolepis*), and snow crab (*Chionoecetes opilio*), in response to a northward shift in the Bering Sea cold pool. They also found that 57% of the variability in commercial snow crab catch is explained by winter sea-ice extent, and a warming climate is the cause of changes in distribution. As the system fluctuates, upper-trophic ice-dependent and ice-associated species will be challenged, and those with restricted ranges and diets will be less resilient than those with greater adaptability (Laidre et al. 2008, Moore and Huntington 2008).

As suggested for marine mammals (Moore and Huntington 2008), some seasonally migrant seabirds may stand to gain from reduced sea ice and an increase in pelagic food sources (e.g. Gall et al. 2012). Crested Auklets (*Aethia cristatella*) appear to have increased their use of the Chukchi Sea in late summer, although the reason is not known; it may be due to improving conditions, population increases, or previous underestimation of use (Maftei and Russ 2014). On the other hand, there is greater evidence of troubling futures for marine birds. Benthic-feeders, such as sea ducks, are likely to lose out. A study by Audubon Alaska and the US Fish and Wildlife Service found that climate models predict a significant decrease in benthic infaunal biomass in waters used by globally significant concentrations of Steller's Eiders (*Polysticta stelleri*), a threatened species under the Endangered Species Act (ESA) (Koeppen et al. 2016). In 2014, an "unprecedented" number (50,000–100,000) of Cassin's Auklets (*Ptychoramphus aleuticus*) washed up on beaches from British Columbia to California (Welch 2015). The recent alarming mass die-off of more than 500,000 Common Murres (*Uria aalge*) in Alaska waters in 2015–2016 initially left scientists puzzled (US Fish and Wildlife Service 2016); it has since been linked to climate change. A redistribution of forage fish in response to a large mass of warm water in the Gulf of Alaska known as "the blob" left the murres starving, with some flying as far inland as Fairbanks in search of food (Farzan 2017). In late 2016, a die-off of several thousand starving Tufted Puffins (*Fratercula cirrhata*) at the Pribilof Islands may also be linked to warmer seas (Welch 2016).

Some marine mammals also face challenges (Laidre et al. 2008, Moore and Huntington 2008). Loss of ice cover on the continental shelf in late summer is a problem for Pacific walrus, which need the ice to haul out and use as a resting platform. When the last of the lingering ice near Hanna Shoal has melted, walrus spend less time foraging and less time hauled out, indicating greater energy expenditure to access food resources due to climate warming (Jay et al. 2017). Additionally, ice seals need sea ice at certain times of the year for whelping, nursing, mating, and molting. There is concern that the changes in the timing of sea-ice availability may affect the ability of ice seals to perform vital life events (Boveng et al. 2009, Cameron et al. 2010, Kelly et al. 2010, Boveng et al. 2013). This has led to an ESA listing of threatened for the Arctic subspecies of ringed seal and the Beringia distinct population segment of bearded seal (*Erignathus barbatus*). Similar concerns led to the listing of the polar bear (*Ursus maritimus*) as threatened (US Fish and Wildlife Service 2015).

Overall, climate is the principal driver of ecological organization, relationships, and changes. While many effects are currently being experienced, many more changes to come are not yet known.

MAPPING METHODS (MAPS 2.3a–p)

We assessed climate using downscaled, four-dimensional, coupled physical/biological models of ocean variables created by NOAA PMEL (Hermann et al. 2013) available from the Alaska Ocean Observing System (AOOS) Arctic Data Portal. Data were available only for the Bering Sea portion of our project area. These projections were based on ocean climate models that pair a Regional Ocean Modeling System (ROMS) with climate model output extracted for the North Pacific from Coupled Model Intercomparison Project 3 (CMIP3) bias-corrected global climate models (GCMs). The downscaled variables have a spatial resolution of 6x6 miles (10x10 km) and many variables also include projections for multiple depth classes (e.g, density of euphausiids in different sections of the water column). Hermann et al. (2013) describe these downscaled models and compare projections from the Canadian Centre for Climate Modelling and Analysis (CCCma) projection model (2003–2040) to the Coordinated Ocean-Ice Reference Experiments (CORE) hindcast climate model (1965–2009) (Large and Yeager 2008).

We selected seven physical and biological variables. Four of the selected variables were assessed by combining multiple depth classes. We analyzed seawater temperature, large microzooplankton, *Neocalanus* (i.e. large neritic copepods), and euphausiids for shallow waters only (0–200 feet [0–60 m] depth); we also analyzed sea water temperature for deep waters (250–650 feet [75–200 m] depth). The other three variables represented surface (sea-ice area fraction, ice phytoplankton) or bottom (benthic infauna) values.

We used the NetCDF Operator Suite to statistically analyze and summarize the time-series data for each model for each 6x6 mile (10x10 km) raster cell. Using the CORE hindcast model, we analyzed all available time steps (weekly) across the entire model time period to summarize average annual values for each variable. Using the CCCma projection model, we compared the recent time period (26 January 2003 to 30 December 2012) to a future time period (6 January 2030 to 4 December 2039) within the model, summarizing total anticipated change from recent conditions to 2040.

Data Quality

For both hindcast and projection, we used a single GCM and have not expressed uncertainty based on variability among models. Models did not include variables related to fish which is a major limiting factor in understanding coming changes in Bering Sea ecology. For an in-depth discussion of the models and their limitations, see Hermann et al. (2013).

Reviewer

• Jeremy Littell

MAP DATA SOURCES

Hindcast and Projection Summaries: Smith and Koeppen (2016) based on Hermann et al. (2013)

Climate

Map Authors: Melanie Smith and Will Koeppen
Cartographer: Daniel P. Huffman

Shallow Sea Water Temperature 0–200 feet (0–60 m)

Annual Average (1965–2009)

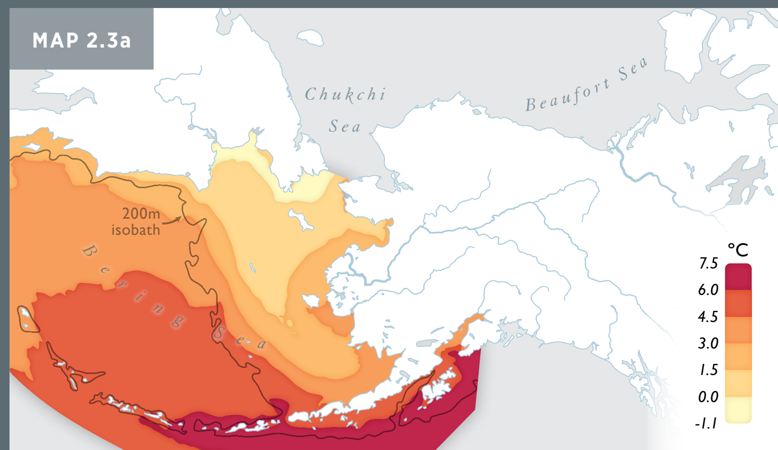

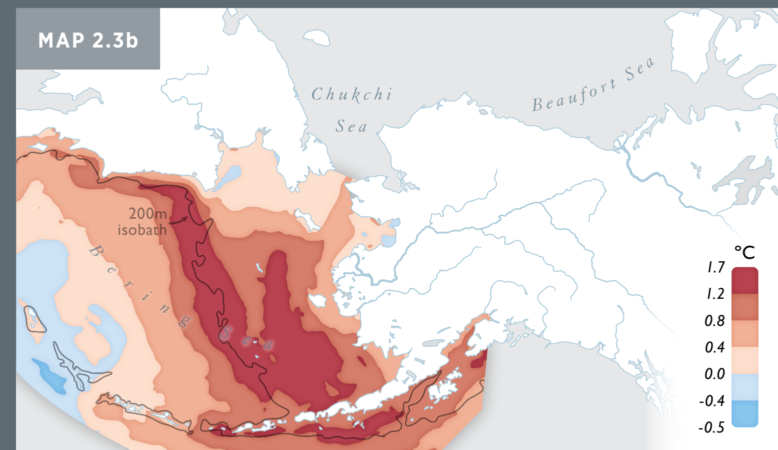

Total Projected Change by 2040

Deep Sea Water Temperature 250–650 feet (75–200 m)

Annual Average (1965–2009)

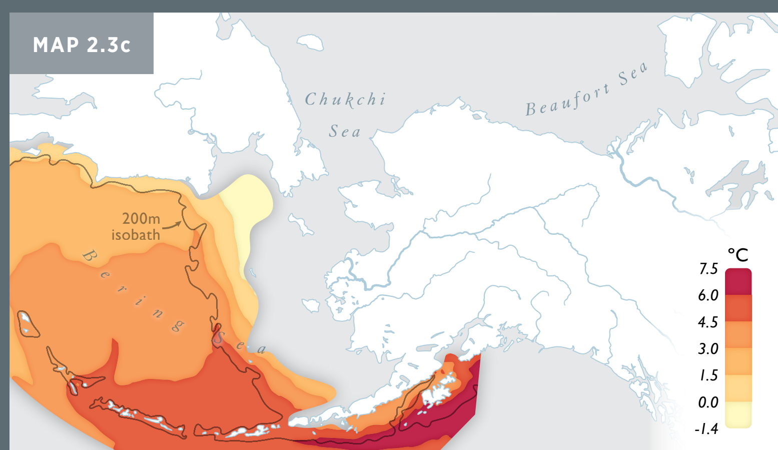

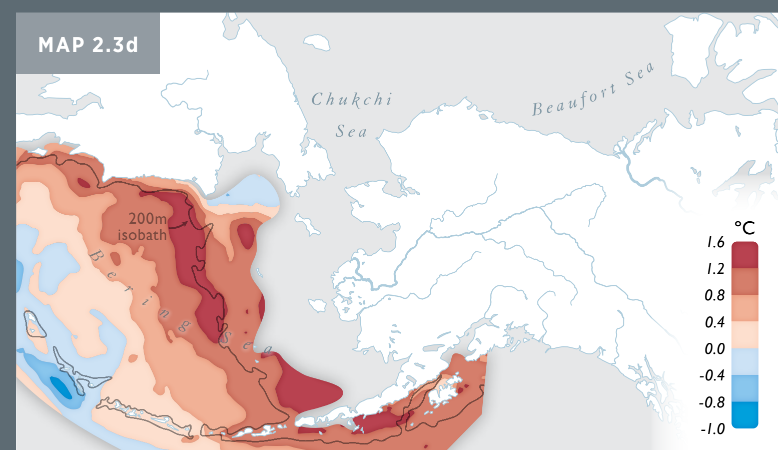

Total Projected Change by 2040

Sea Ice Concentration

Annual Average (1965–2009)

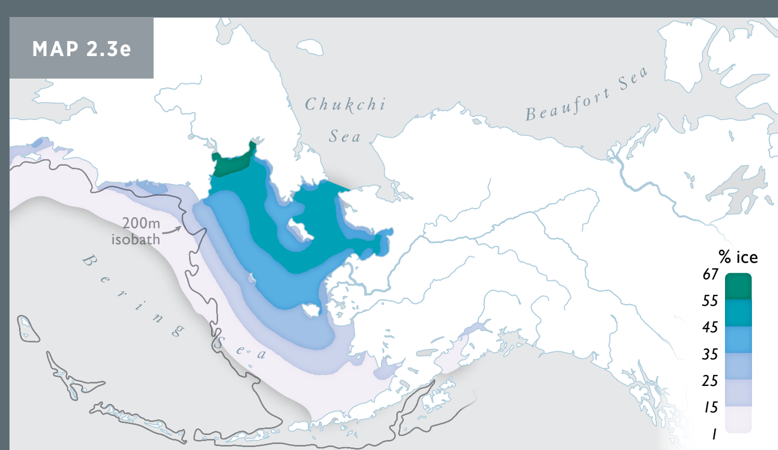

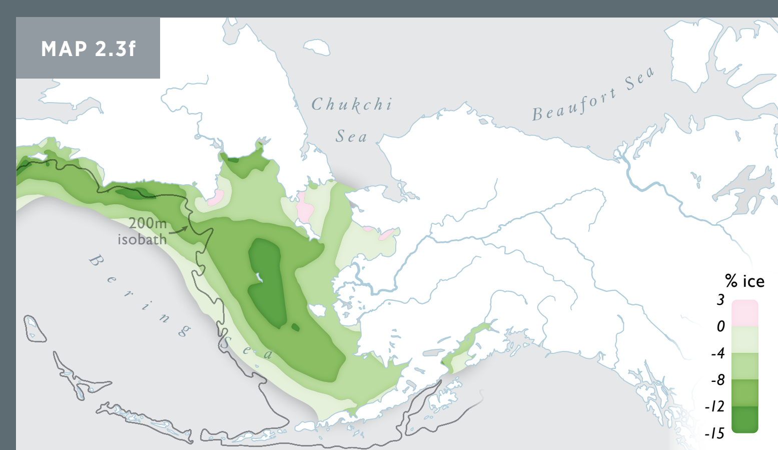

Total Projected Change by 2040

Ice Phytoplankton Concentration

Annual Average (1965–2009)

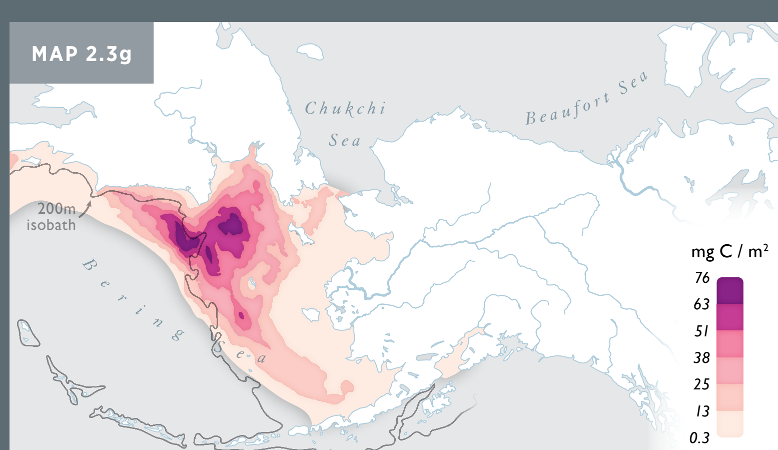

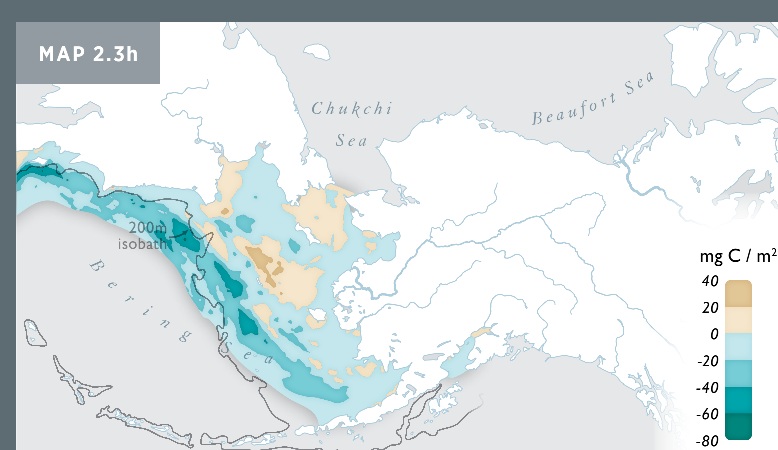

Total Projected Change by 2040

Audubon ALASKA

Microzooplankton Concentration 0–200 feet (0–60 m)

Annual Average (1965–2009)

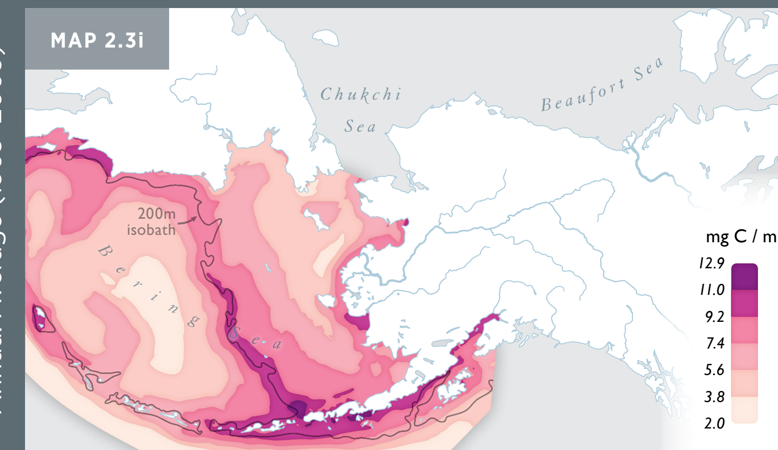

Total Projected Change by 2040

Large Neritic Copepod Concentration 0–200 feet (0–60 m)

Annual Average (1965–2009)

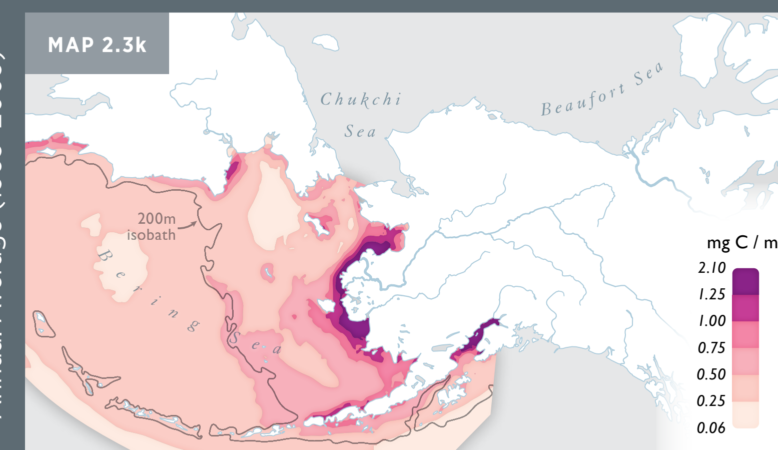

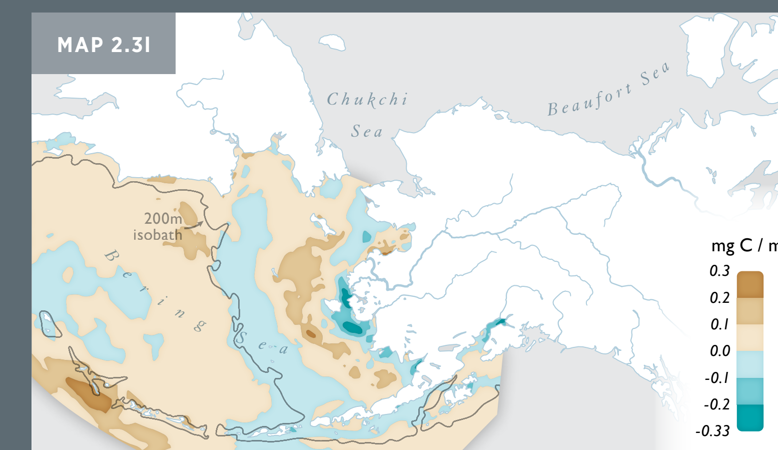

Total Projected Change by 2040

Euphausiid Concentration 0–200 feet (0–60 m)

Annual Average (1965–2009)

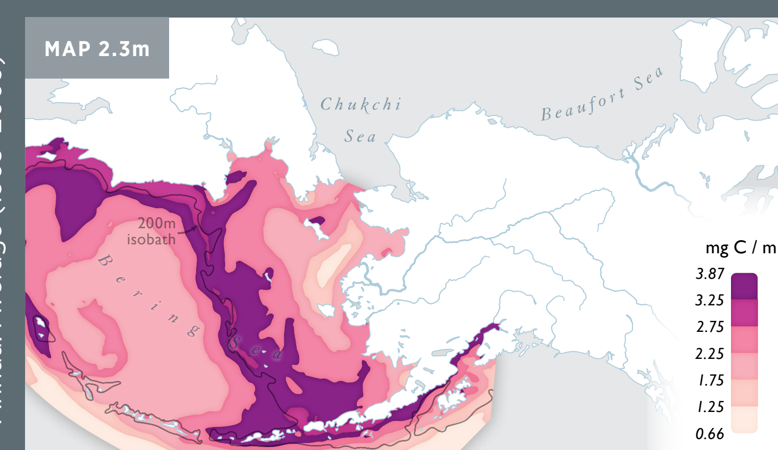

Total Projected Change by 2040

Benthic Infaunal Biomass Concentration

Annual Average (1965–2009)

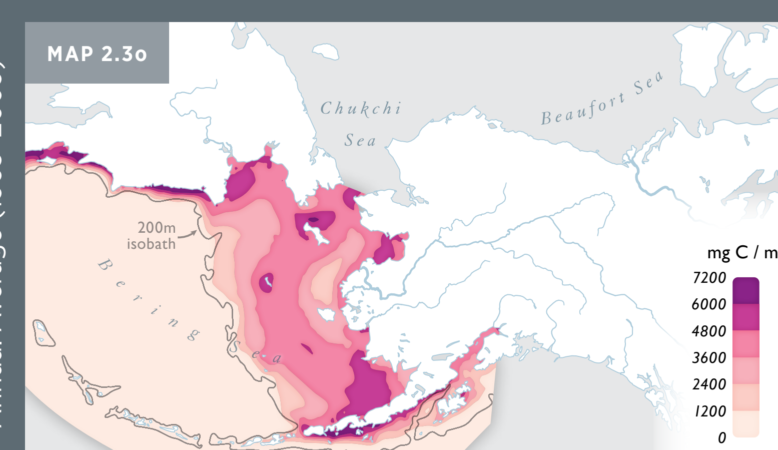

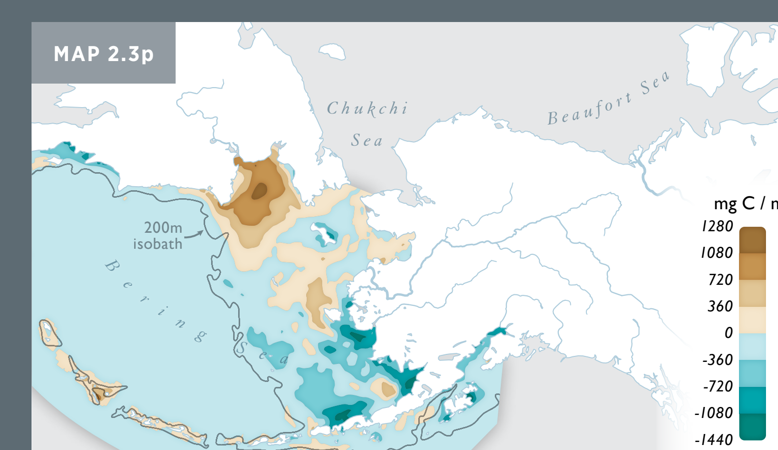

Total Projected Change by 2040

Smith and Koeppen (2016) [based on Hermann et al. (2013)]

A Closer Look: Bering Sea Weather

Max Goldman

The weather of the Bering Sea changes dramatically on time scales ranging from days to decades (Overland et al. 1999). These changes are closely tied to the physical properties of the ocean, resulting in variations and fluctuations in the marine populations (Overland and Stabeno 2004). By evaluating the nature of weather in the Bering Sea, we can gain an understanding of how this environment influences, and is influenced by, patterns and fluctuations in the global seascape.

The Bering Sea is one of the stormiest places on the planet through much of the winter, with three to five storms per month during the winter, and gale-force winds that occasionally push sea surface heights up to 40 feet (12 m) (Stabeno et al. 2001, Bond 2005). Although the nature of these storms is highly variable, there are basically two types that typify Bering Sea weather, and perpetuate the systems within. One of the common Bering Sea storms includes an atmospheric circulation pattern moving in from lower latitudes, which produces repeated systems of tight rotation and low-pressure, typically resulting in high winds and moderate temperatures (Bond 2005). This common pattern is perpetuated by the North Pacific High, a high-pressure system generally occurring in summer months between Hawaii and California that leads to Arctic sea-ice retreat.

The other common circulation pattern brings intense bouts of Arctic air from the north during the winter, which pushes the ice-edge south with cold air temperatures (Weeks 2010) and high winds. This pattern is perpetuated by the Aleutian Low (Figure 2.4-3), a seasonal low-pressure system located near the Aleutian Islands in winter that is one of the largest atmospheric circulation patterns in the Northern Hemisphere (Rodionov et al. 2005, Rodionov et al. 2007). Because the typical direction of winds associated with this system has undergone no substantial change in recent decades, winter sea-ice extent in the Bering Sea has also remained relatively steady over the satellite record (1979–present) (National Snow and Ice Data Center 2016, Walsh et al. 2017, Gan et al. 2017).

The Bering Sea ice cover is driven by atmospheric circulation and can be compared to a "conveyor belt," as sea ice forms in the northern Bering Sea and is pushed south by northerly winds (Pease 1980, Weeks 2010). Where it contacts warm shelf waters, the ice melts and cools the water column, facilitating further sea-ice advance. The winds in winter reflect the location of storms associated with the Aleutian Low pressure system. When storm tracks are displaced to the east, winds over the Bering Sea shelf are more northerly, driving expanded sea-ice extent (Bond 2005, Rodionov et al. 2007).

The annual or decadal winter weather conditions in the Bering Sea depend on the tendency for one type of pattern versus the other (Overland et al. 1999, Bond 2005). Many factors, known and unknown, feed the propensity for one system over the other, and long time scales can be dominated by warmer or colder systems. The early 1970s were dominated by colder winds from the north and extensive, long-lasting ice packs. This period was followed by a warm period of reduced ice cover from the late 1970s through much of the 1980s. For example, at St. Paul in the Pribilof Islands, the average winter air temperatures warmed 14.5° F (8° C) during this transition (Reynolds and Smith 1994). This cyclical, decadal shift in weather/climate regimes is known as the Pacific Decadal Oscillation, or PDO. Even when accounting for the PDO, the winters of recent decades have been warmer than normal on average (see Climate Summary), with earlier sea-ice retreat, diminishing multiyear pack ice, and later freeze-up.

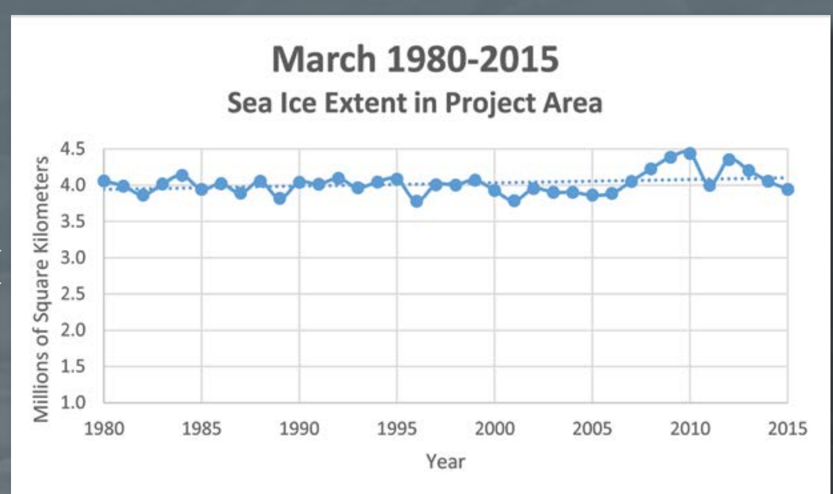

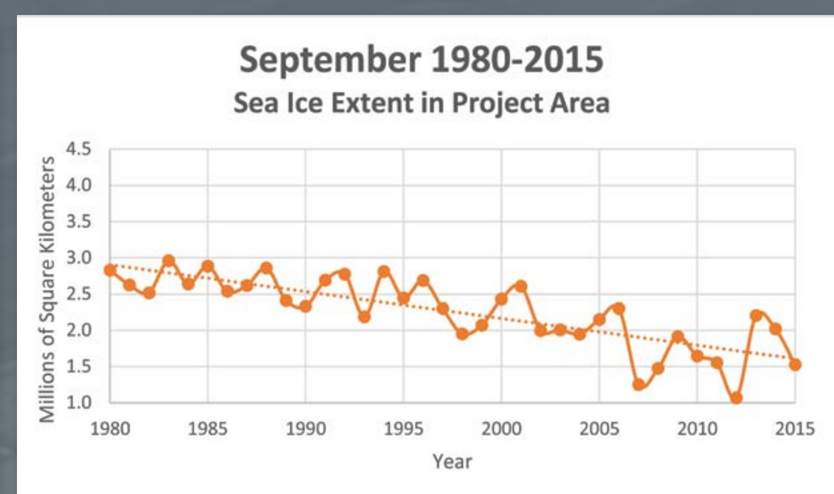

Based on data from Fetterer et al. (2016).

FIGURES 2.4-1 (LEFT), 2.4-2 (RIGHT). The graphs show average March and September sea ice extent (millions of square kilometers) within the project area for each year between 1980 and 2015. March sea ice extent has remained relatively constant over this time period, while September sea ice extent has decreased.

Tim Sullivan / USCG

Map Author: Max Goldman
Cartographer: Daniel P. Huffman

Audubon ALASKA

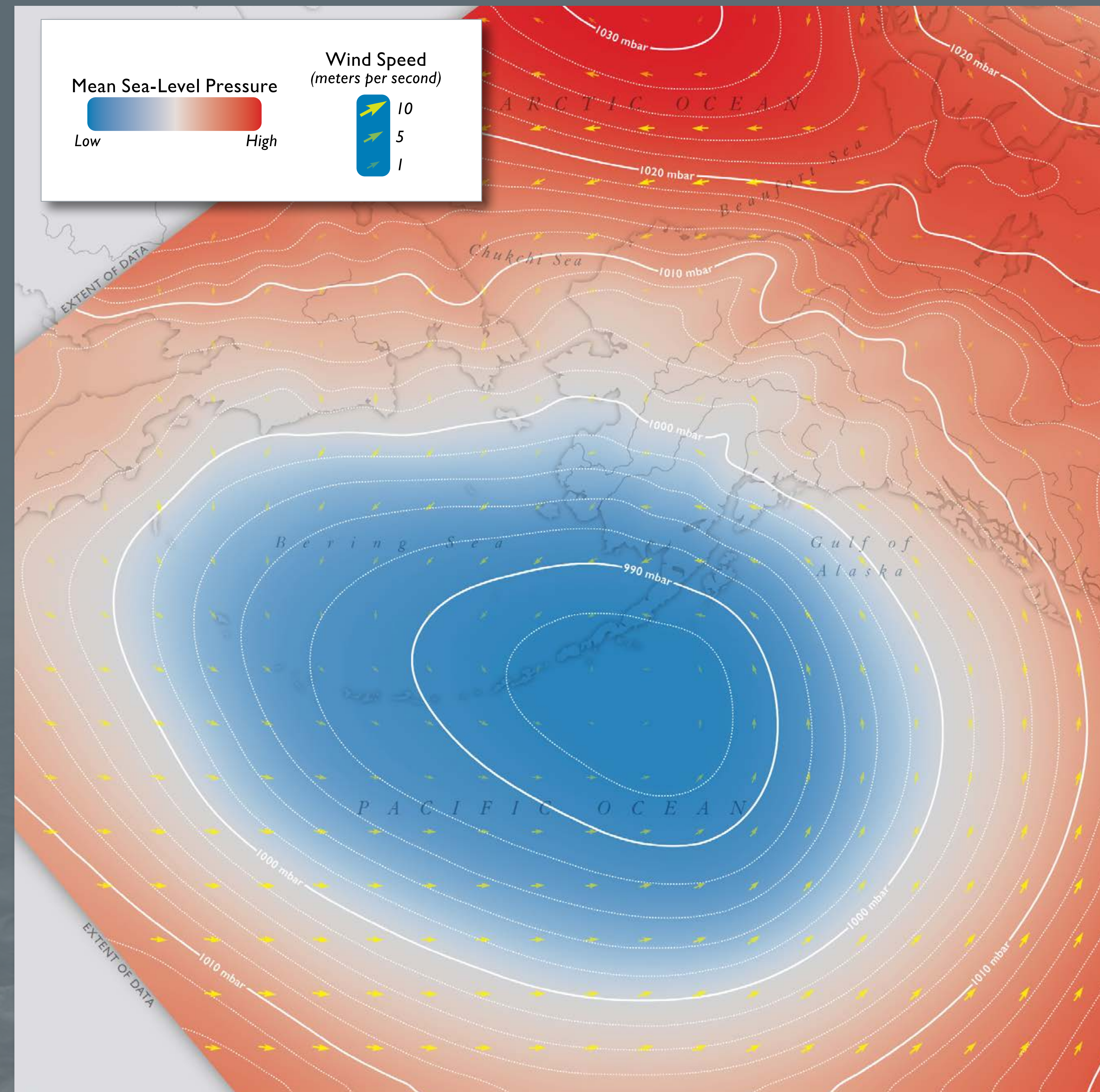

Based on data from NOAA Earth System Research Laboratory-Physical Sciences Division (2017).

FIGURE 2.4-3. ALEUTIAN LOW-PRESSURE SYSTEM

Among the stormiest places on the planet, winter weather in the Bering Sea is driven in large part by a semipermanent, low-pressure system called the Aleutian Low. This map shows an example of that system from February of 2016, illustrating the area of low pressure situated over the Aleutian Island chain. The Aleutian Low produces heavy rain and strong, cyclonic winds that push sea ice, formed annually in the colder, northern part of the Bering Sea, southwest over the Bering shelf.

REFERENCES

Abelmann, A., R. Gersonde, G. Knorr, X. Zhang, B. Chapligin, E. Maier, O. Esper, H. Friedrichsen, G. Lohmann, and H. Meyer. 2015. The seasonal sea-ice zone in the glacial Southern Ocean as a carbon sink. *Nature Communications* 6.

Arctic Climate Impact Assessment. 2004. Impacts of a Warming Arctic: Arctic Climate Impact Assessment. Cambridge University Press, Cambridge, United Kingdom.

Aksenov, Y., V. V. Ivanov, A. J. G. Nurser, S. Bacon, I. V. Polyakov, A. C. Coward, A. C. Naveira-Garabato, and A. Beszczynska-Moeller. 2011. The Arctic Circumpolar Boundary Current. *Journal of Geophysical Research Atmospheres* 116:C09017.

Amstrup, S. C., B. G. Marcot, and D. C. Douglas. 2008. A Bayesian network modeling approach to forecasting the 21st century worldwide status of polar bears, *In Arctic Sea Ice Decline: Observations, Projections, Mechanisms, and Implications*. pp. 213-268. American Geophysical Union, Washington, DC.

Arctic Monitoring and Assessment Programme. 1998. AMAP Assessment Report: Arctic Pollution Issues. Arctic Monitoring and Assessment Programme, Oslo, Norway.

Audubon Alaska. 2009. Recurring Leads (Average Extent 1993-2004) GIS File. Audubon Alaska, Anchorage, AK.

______. 2016a. Distribution of $\delta^{13}C$ in Surface Sediments GIS file. Audubon Alaska, Anchorage, AK.

______. 2016b. Landfast Ice GIS File. Audubon Alaska, Anchorage, AK.

______. 2016c. Monthly Sea Ice Approximate 2006-2015 Medians GIS File. Audubon Alaska, Anchorage, AK.

______. 2016d. Southernmost Ice Extent GIS File. Anchorage, AK.

Audubon Alaska, Kawerak, and Sandhill.Culture.Craft. 2017. Traditional Knowledge-Holder Map Review Workshop. February 21-22, 2017. Nome, AK.

Benke, A. C. and C. E. Cushing. 2005. *Rivers of North America*. Elsevier Academic Press, Burlington, MA.

Bond, A. L., I. L. Jones, S. S. Seneviratne, and S. B. Muzaffar. 2013. Least Auklet (*Aethia pusilla*), *In The Birds of North America Online*. P. G. Rodewald ed. Cornell Lab of Ornithology, Ithaca, NY. Accessed online at https://birdsna.org/Species-Account/bna/species/leauk/introduction.

Bond, N. A. 2005. What differences have occurred in summer and winter weather in the Bering Sea in the past 30 years? National Oceanic and Atmospheric Administration. Accessed online 20 May 2017 at http://www.beringclimate.noaa.gov/essays_bond.html.

Bouttes, N., D. Paillard, and D. M. Roche. 2010. Impact of brine-induced stratification on the glacial carbon cycle. *Climate of the Past* 6:575-589.

Boveng, P. L., J. L. Bengtson, T. W. Buckley, M. F. Cameron, S. P. Dahle, B. P. Kelly, B. A. Megrey, J. E. Overland, and N. J. Williamson. 2009. Status Review of the Spotted Seal (*Phoca largha*). NOAA Technical Memorandum NMFS-AFSC-200. US Department of Commerce, National Oceanic and Atmospheric Administration, Seattle, WA.

Boveng, P. L., J. L. Bengtson, M. F. Cameron, S. P. Dahle, E. A. Logerwell, J. M. London, J. E. Overland, J. T. Sterling, D. E. Stevenson, B. L. Taylor, and H. L. Ziel. 2013. Status Review of the Ribbon Seal (*Histriophoca fasciata*). NOAA Technical Memorandum NMFS-AFSC-255. National Oceanic and Atmospheric Administration, Seattle, WA.

Bradstreet, M. S. W. and W. E. Cross. 1982. Trophic relationships at high Arctic ice edges. *Arctic* 35:1-12.

Brugler, E. T., R. S. Pickart, G. W. K. Moore, S. Roberts, T. J. Weingartner, and H. Statscewich. 2014. Seasonal to interannual variability of the Pacific water boundary current in the Beaufort Sea. *Progress in Oceanography* 127:1-20.

Calbet, A. 2008. The trophic roles of microzooplankton in marine systems. *ICES Journal of Marine Science* 65:325-331.

Cameron, M. F., J. L. Bengtson, P. L. Boveng, J. Jansen, B. P. Kelly, S. Dahle, E. Logerwell, J. Overland, C. Sabine, and G. Waring. 2010. Status Review of the Bearded Seal (*Erignathus barbatus*). NOAA Technical Memorandum NMFS-AFSC-211. National Oceanic and Atmospheric Administration, Seattle, WA.

Carmack, E. C. and R. W. MacDonald. 2002. Oceanography of the Canadian Shelf of the Beaufort Sea: A setting for marine life. *Arctic* 55:29-45.

Coachman, L. K., K. Aagaard, and R. B. Tripp. 1975. *Bering Strait: The Regional Physical Oceanography*. University of Washington Press, Seattle, WA.

Conover, R. J. 1988. Comparative life histories in the genera *Calanus* and *Neocalanus* in high latitudes of the northern hemisphere. *Hydrobiologia* 167:127-142.

Divoky, G. J. 1979. Sea ice as a factor in seabird distribution and ecology in the Beaufort, Chukchi, and Bering Seas, *In Conservation of Marine Birds of Northern North America. Wildlife Research Report No. 11*. J. C. Bartonek and D. N. Nettleship eds. US Fish and Wildlife Service, Washington, DC.

Dunton, K. H., S. V. Schonberg, and L. W. Cooper. 2012. Food web structure of the Alaskan nearshore shelf and estuarine lagoons of the Beaufort Sea. *Estuaries and Coasts* 35:416-435.

Eicken, H., L. Shapiro, A. G. Gaylord, A. Mahoney, and P. W. Cotter. 2009. Recurring Spring Leads and Landfast Ice in the Beaufort and Chukchi Seas, 1993–2004. National Snow and Ice Data Center, Boulder, CO.

______. 2005. Mapping and Characterization of Recurring Spring Leads and Landfast Ice in the Beaufort and Chukchi Seas. Minerals Management Service, Alaska OCS Region, Anchorage, AK.

Elphick, C. S. and G. L. Hunt. 1993. Variations in the distributions of marine birds with water mass in the northern Bering Sea. *Condor* 95:33-44.

Farzan, S. 2017. Murre Die-Off Linked To Warm Water Temperatures. KBBI, Homer, AK.

Fetterer, F., K. Knowles, W. Meier, and M. Savoie. 2016. Sea Ice Index, Version 2. National Snow and Ice Data Center, Boulder, CO.

Gall, A. E., R. H. Day, and T. J. Weingartner. 2013. Structure and variability of the marine-bird community in the northeastern Chukchi Sea. *Continental Shelf Research* 67:96-115.

Gan, B., L. Wu, F. Jia, S. Li, W. Cai, H. Nakamura, M. A. Alexander, and A. J. Miller. 2017. On the response of the Aleutian Low to greenhouse warming. *Journal of Climate* 30:3907-3925.

Gradinger, R. 2008. Sea ice, *In Arctic Ocean Synthesis: Analysis of Climate Change Impacts in the Chukchi and Beaufort Seas with Strategies for Future Research*. R. Hopcroft, B. Bluhm, and R. Gradinger eds. University of Alaska Fairbanks, Institute of Marine Science, Fairbanks, AK.

Grebmeier, J. M., L. W. Cooper, C. A. Ashjian, B. A. Bluhm, R. B. Campbell, K. E. Dunton, J. Moore, S. Okkonen, G. Sheffield, J. Trefry, and S. Y. Pasternak. 2015. Pacific Marine Arctic Regional Synthesis (PacMARS) Final Report. North Pacific Research Board, Anchorage, AK.

Grebmeier, J. M., L. W. Cooper, H. M. Feder, and B. I. Sirenko. 2006. Ecosystem dynamics of the Pacific-influenced northern Bering and Chukchi Seas in the Amerasian Arctic. *Progress in Oceanography* 71:331-361.

Hermann, A. J., G. A. Gibson, N. A. Bond, E. N. Curchitser, K. Hedstrom, W. Cheng, M. Wang, P. J. Stabeno, L. Eisner, and K. D. Cieciel. 2013. A multivariate analysis of observed and modeled biophysical variability on the Bering Sea shelf: Multidecadal hindcasts (1970–2009) and forecasts (2010–2040). *Deep Sea Research Part II: Topical Studies in Oceanography* 94:121-139.

Horner, R. and G. C. Schrader. 1982. Relative contributions of ice algae, phytoplankton, and benthic microalgae to primary production in nearshore regions of the Beaufort Sea. *Arctic* 35:485-503.

Hunt, G. L., P. Stabeno, G. Walters, E. Sinclair, R. D. Brodeur, J. M. Napp, and N. A. Bond. 2002. Climate change and control of the southeastern Bering Sea pelagic ecosystem. *Deep Sea Research Part II: Topical Studies in Oceanography* 49:5821-5853.

Jay, C. V., R. L. Taylor, A. S. Fischbach, M. S. Udevitz, and W. S. Beatty. 2017. Walrus haul-out and in water activity levels relative to sea ice availability in the Chukchi Sea. *Journal of Mammalogy* 98:386-396.

Johnson, M. and H. Eicken. 2016. Estimating Arctic sea-ice freeze-up and break-up from the satellite record: A comparison of different approaches in the Chukchi and Beaufort Seas. *Elementa Science of the Anthropocene* 4:124.

Kelly, B. P., J. L. Bengtson, P. L. Boveng, M. F. Cameron, S. P. Dahle, J. K. Jansen, E. A. Logerwell, J. E. Overland, C. L. Sabine, and G. T. Waring. 2010. Status Review of the Ringed Seal (*Phoca hispida*). NOAA Technical Memorandum NMFS-AFSC-212. National Oceanic and Atmospheric Administration, Springfield, VA.

Koeppen, W., K. Kuletz, A. Poe, H. Renner, M. Smith, T. Van Pelt, N. Walker, and J. Williams. 2016. Chapter 6: Exploring vulnerabilities of seabirds using projected changes in climate in the Aleutian Islands and Bering Sea, *In The Aleutian-Bering Climate Vulnerability Assessment. Final Report*. A. Poe, T. Van Pelt, and J. Littell eds. Aleutian and Bering Sea Islands Landscape Conservation Cooperative, Anchorage, AK.

Ladd, C., J. Jahncke, G. L. Hunt, K. O. Coyle, and P. J. Stabeno. 2005. Hydrographic features and seabird foraging in Aleutian passes. *Fisheries Oceanography* 14:178-195.

Laidre, K. L., H. Stern, K. M. Kovacs, L. F. Lowry, S. E. Moore, E. V. Regehr, S. H. Ferguson, O. Wiig, P. Boveng, R. P. Angliss, E. W. Born, D. Litovka, L. T. Quakenbush, C. Lydersen, D. Vongraven, and F. Ugarte. 2015. Arctic marine mammal population status, sea ice habitat loss, and conservation recommendations for the 21st century. *Conservation Biology* 29:724-737.

Laidre, K. L., I. Stirling, L. F. Lowry, Ø. Wiig, M. P. Heide-Jørgensen, and S. H. Ferguson. 2008. Quantifying the sensitivity of Arctic marine mammals to climate-induced habitat change. *Ecological Applications* 18:S97-S125.

Large, W. G. and S. G. Yeager. 2008. The global climatology of an interannually varying air-sea flux dataset. *Climate Dynamics* 33:341-364.

Llinás, L., R. S. Pickart, J. T. Mathis, and S. L. Smith. 2009. Zooplankton inside an Arctic Ocean cold-core eddy: Probable origin and fate. *Deep Sea Research Part II: Topical Studies in Oceanography* 56:1290-1304.

Maftei, M. and R. Russ. 2014. A mass post-breeding movement of Crested Auklets *Aethia cristatella* in the Chukchi Sea. *Marine Ornithology* 42:31-34.

Marine Mammal Commission. 2000. Impacts of changes in sea ice and other environmental parameters on marine mammals. Marine Mammal Commission Workshop, Girdwood, AK.

Martello, M. L. 2008. Arctic indigenous peoples as representations and representatives of climate change. *Social Studies of Science* 38:351-376.

Maslanik, J., J. Stroeve, C. Fowler, and W. Emery. 2011. Distribution and trends in Arctic sea ice age through spring 2011. *Geophysical Research Letters* 38:L13502.

McClelland, J. W., R. M. Holmes, B. J. Peterson, P. A. Raymond, R. G. Striegl, A. V. Zhulidov, S. A. Zimov, N. Zimov, S. E. Tank, R. G. M. Spencer, R. Staples, T. Y. Gurtovaya, and C. G. Griffin. 2016. Particulate organic carbon and nitrogen export from major Arctic rivers. *Global Biogeochemical Cycles* 30:629-643.

Meier, W. N., G. K. Hovelsrud, B. E. H. Oort, J. R. Key, K. M. Kovacs, C. Michel, C. Haas, M. A. Granskog, S. Gerland, and D. K. Perovich. 2014. Arctic sea ice in transformation: A review of recent observed changes and impacts on biology and human activity. *Reviews of Geophysics* 52:185-217.

Moline, M. A., N. J. Karnovsky, Z. Brown, G. J. Divoky, T. K. Frazer, C. A. Jacoby, J. J. Torres, and W. R. Fraser. 2008. High latitude changes in ice dynamics and their impact on polar marine ecosystems. *Annals of the New York Academy of Sciences* 1134:267-319.

Moller, H., F. Berkes, P. O. B. Lyver, and M. Kislalioglu. 2004. Combining science and traditional ecological knowledge: monitoring populations for co-management. *Ecology and Society* 9:2.

Moore, S. E. and H. P. Huntington. 2008. Arctic marine mammals and climate change: Impacts and resilience. *Ecological Applications* 18:S157-S165.

Mueter, F. J. and M. A. Litzow. 2008. Sea ice retreat alters the biogeography of the Bering Sea continental shelf. *Ecological Applications* 18:309-320.

National Oceanic and Atmospheric Administration. 1988. Bering, Chukchi, and Beaufort Seas Coastal and Ocean Zones: Strategic Assessment Data Atlas. National Oceanic and Atmospheric Administration, Rockville, MD.

______. 2006. Review of the Status of the Right Whales in the North Atlantic and North Pacific Oceans. National Oceanic and Atmospheric Administration Alaska Regional Office, Juneau, AK.

______. 2017. Ocean Currents. National Oceanic and Atmospheric Administration. Accessed online 15 April 2017 at http://www.noaa.gov/resource-collections/ocean-currents.

National Oceanic and Atmospheric Administration Earth System Research Laboratory—Physical Sciences Division. 2017. NCEP North American Regional Reanalysis. National Oceanic and Atmospheric Administration, Boulder, CO. Accessed online at https://www.esrl.noaa.gov/psd/data/gridded/data.narr.html.

National Snow and Ice Data Center. 2016. IMS Daily Northern Hemisphere Snow and Ice Analysis at 4 km and 24 km Resolution. National Snow and Ice Data Center, Boulder, CO. Accessed online at http://nsidc.org/data/docs/noaa/g02156_ims_snow_ice_analysis/index.html#acq_proc.

National Snow and Ice Data Center, F. Fetterer, and C. Fowler. 2006. National Ice Center Arctic Sea Ice Charts and Climatologies in Gridded Format. National Snow and Ice Data Center, Boulder, CO.

National Snow and Ice Data Center and C. S. Konig Beatty. 2012. Arctic Landfast Sea Ice 1953-1998, Version 1. National Snow and Ice Data Center, Boulder, CO.

Nihoul, J. C. J., P. Adam, P. Brasseur, E. Deleersnijder, S. Djenidi, and J. Haus. 1993. Three-dimensional general circulation model of the northern Bering Sea's summer ecohydrodynamics. *Continental Shelf Research* 13:509-542.

Nikolopoulos, A., R. S. Pickart, P. S. Fratantoni, K. Shimada, D. J. Torres, and E. P. Jones. 2009. The western Arctic boundary current at 152°W: Structure, variability, and transport. *Deep Sea Research Part II: Topical Studies in Oceanography* 56:1164-1181.

Oceana and Kawerak. 2014. Bering Strait Marine Life and Subsistence Use Data Synthesis. Oceana and Kawerak, Juneau, AK.

Overland, J. E., J. M. Adams, and N. A. Bond. 1999. Decadal variability of the Aleutian Low and its relation to high-latitude circulation. *Journal of Climate* 12:1542-1548.

Overland, J. E. and P. J. Stabeno. 2004. Is the climate of Bering Sea warming and affecting the ecosystem? *EOS* 85:309-316.

Parrenin, F., V. Masson-Delmotte, P. Köhler, D. Raynaud, D. Paillard, J. Schwander, C. Barbante, A. Landais, A. Wegner, and J. Jouzel. 2013. Synchronous change of atmospheric CO_2 and Antarctic temperature during the last deglacial warming. *Science* 339:1060-1063.

Pease, C. H. 1980. Eastern Bering Sea ice processes. *Monthly Weather Review* 108:2015-2023.

Perovich, D. K., S. Gerland, S. Hendricks, W. Meier, M. Nicolaus, J. A. Richter-Menge, and M. Tschudi. 2013. Sea ice, *In Arctic Report Card 2013*. M. O. Jeffries, J. A. Richter-Menge, and J. E. Overland eds. Accessed online at http://www.arctic.noaa.gov/reportcard.

Perovich, D. K., S. Gerland, S. Hendricks, W. N. Meier, M. Nicolaus, and M. Tschudi. 2015. The Arctic: Sea ice cover [in "State of the Climate 2014"]. *Bulletin of the American Meteorological Society* 96:S145-S146.

Perovich, D. K. and J. A. Richter-Menge. 2015. Regional variability in sea ice melt in a changing Arctic. *Philosophical Transactions of the Royal Society of London A: Mathematical, Physical and Engineering Sciences* 373:20140165.

Piatt, J. F. and A. M. Springer. 2007. Marine ecoregions of Alaska, *In Long-term Ecological Change in the Northern Gulf of Alaska*. R. B. Spies ed., pp. 522–526. Elsevier, Amsterdam, Netherlands.

Pickart, R. and B. Corlett. 2016. Closing the mass budget between Bering Strait and the Arctic Basin: The Chukchi slope current. *In Alaska Marine Science Symposium*. Anchorage, AK.

Pickart, R. S., G. W. K. Moore, D. J. Torres, P. S. Fratantoni, R. A. Goldsmith, and J. Yang. 2009. Upwelling on the continental slope of the Alaskan Beaufort Sea: Storms, ice, and oceanographic response. *Journal of Geophysical Research: Oceans* 114:C00A13.

Pickart, R. S., L. M. Schulze, G. W. K. Moore, M. A. Charette, K. R. Arrigo, G. van Dijken, and S. L. Danielson. 2013. Long-term trends of upwelling and impacts on primary productivity in the Alaskan Beaufort Sea. *Deep Sea Research Part I: Oceanographic Research Papers* 79:106-121.

Pickart, R. S., M. A. Spall, G. W. K. Moore, T. J. Weingartner, R. A. Woodgate, K. Aagaard, and K. Shimada. 2011. Upwelling in the Alaskan Beaufort Sea: Atmospheric forcing and local versus non-local response. *Progress in Oceanography* 88:78-100.

Pisareva, M. N., R. S. Pickart, M. A. Spall, C. Nobre, D. J. Torres, G. W. K. Moore, and T. E. Whitledge. 2015. Flow of Pacific water in the western Chukchi Sea: Results from the 2009 RUSALCA expedition. *Deep Sea Research Part I: Oceanographic Research Papers* 105:53-73.

Raymond-Yakoubian, J., Y. Khokhlov, and A. Yarzutkina. 2014. Indigenous Knowledge and Use of Bering Strait Region Ocean Currents. Kawerak, Inc., Nome, AK.

Reed, R. K. and P. J. Stabeno. 1997. Long-term measurements of flow near the Aleutian Islands. *Journal of Marine Research* 55:565-575.

Reynolds, R. W. and T. M. Smith. 1994. Improved global sea surface temperature analyses using optimum interpolation. *Journal of Climate* 7:929-948.

Rode, K. D., E. V. Regehr, D. C. Douglas, G. Durner, A. E. Derocher, G. W. Thiemann, and S. M. Budge. 2014. Variation in the response of an Arctic top predator experiencing habitat loss: Feeding and reproductive ecology of two polar bear populations. *Global Change Biology* 20:76-88.

Rodionov, S. N., N. A. Bond, and J. E. Overland. 2007. The Aleutian Low, storm tracks, and winter climate variability in the Bering Sea. *Deep Sea Research Part II: Topical Studies in Oceanography* 54:2560-2577.

Rodionov, S. N., J. E. Overland, and N. A. Bond. 2005. The Aleutian Low and winter climatic conditions in the Bering Sea. Part I: Classification. *Journal of Climate* 18:160-177.

Sapozhnikov, V. V., O. S. Ivanova, and N. V. Mordasova. 2011. Identification of local upwelling zones in the Bering Sea using hydrochemical parameters. *Oceanology* 51:247-254.

Satterthwaite-Phillips, D., C. Krenz, G. Gray, and L. Dodd. 2016. Iñuuniałiqput Iḷiḷugu Nunaŋŋuanun: Documenting Our Way of Life through Maps. Northwest Arctic Borough, Kotzebue, AK.

Scenarios Network for Alaska and Arctic Planning. 2016. Historical Sea Ice Atlas: Observed Estimates of Sea Ice Concentration in Alaska Waters. University of Alaska Fairbanks. Accessed online at http://ckan.snap.uaf.edu/dataset/historical-sea-ice-atlas-observed-estimates-of-sea-ice-concentration-in-alaska-waters.

Schmoker, C., S. Hernández-León, and A. Calbet. 2013. Microzooplankton grazing in the oceans: Impacts, data variability, knowledge gaps and future directions. *Journal of Plankton Research* 35:691-706.

Schonberg, S. V., J. T. Clarke, and K. H. Dunton. 2014. Distribution, abundance, biomass and diversity of benthic infauna in the northeast Chukchi Sea, Alaska: Relation to environmental variables and marine mammals. *Deep Sea Research Part II: Topical Studies in Oceanography* 102:144-163.

Sigler, M. F., M. Renner, S. L. Danielson, L. B. Eisner, R. R. Lauth, K. J. Kuletz, E. A. Logerwell, and G. L. Hunt, Jr. 2011. Fluxes, fins, and feathers: Relationships among the Bering, Chukchi, and Beaufort Seas in a time of climate change. *Oceanography* 24:250-265.

Sigman, D. M., M. P. Hain, and G. H. Haug. 2010. The polar ocean and glacial cycles in atmospheric CO_2 concentration. *Nature* 466:47-55.

Smith, M. A. and W. Koeppen. 2016. Analysis of PMEL Models CORE and CCCma to Summarize Past and Future Conditions in the Bering Sea. Audubon Alaska and Axiom Data Science, Anchorage, AK.

Spall, M. A., R. S. Pickart, P. S. Fratantoni, and A. J. Plueddemann. 2008. Western Arctic shelfbreak eddies: Formation and transport. *Journal of Physical Oceanography* 38:1644-1668.

Spiridonov, V. A., M. V. Gavrilo, E. D. Krasnova, and N. G. Nikolaeva. 2011. Atlas of Marine and Coastal Biological Diversity of the Russian Arctic. WWF Russia, Moscow, Russia.

Springer, A. M. and C. P. McRoy. 1993. The paradox of pelagic food webs in the northern Bering Sea—III: Patterns of primary production. *Continental Shelf Research* 13:575-599.

Stabeno, P. J., N. A. Bond, N. B. Kachel, S. A. Salo, and J. D. Schumacher. 2001. On the temporal variability of the physical environment over the south-eastern Bering Sea. *Fisheries Oceanography* 10:81-98.

Stabeno, P. J., J. D. Schumacher, and K. Ohtani. 1999. The physical oceanography of the Bering Sea, *In Dynamics of the Bering Sea: A Summary of Physical, Chemical, and Biological Characteristics, and a Synopsis of Research on the Bering Sea*. T. R. Loughlin and K. Ohtani eds. North Pacific Marine Science Organization (PICES), University of Alaska Sea Grant AK-SG-99-03, Fairbanks, AK.

Stringer, W. J. and J. E. Groves. 1991. Location and areal extent of polynyas in the Bering and Chukchi Seas. *Arctic* 44:164-171.

Sun, X. and K. Matsumoto. 2010. Effects of sea ice on atmospheric pCO_2: A revised view and implications for glacial and future climates. *Journal of Geophysical Research: Biogeosciences* 115:G02015.

Takahashi, K., A. C. Ravelo, C. A. Alvarez Zarikian, and Expedition 323 Scientists. 2011. Expedition 323 Summary. Proceedings of the Integrated Ocean Drilling Program (IODP).

Tschudi, M., C. Fowler, and J. Maslanik. 2015. EASE-Grid Sea Ice Age, Version 2. NASA National Snow and Ice Data Center Distributed Active Archive Center, Boulder, CO. Accessed online at http://nsidc.org/data/docs/daac/nsidc0611-sea-ice-age/.

Tschudi, M., C. Fowler, J. Maslanik, and J. Stroeve. 2010. Tracking the movement and changing surface characteristics of Arctic sea ice. *IEEE Journal of Selected Topics in Applied Earth Observations and Remote Sensing* 3:536-540.

University of Alaska Fairbanks Institute of Marine Science. 2009. Chukchi Sea Circulation. Accessed online at http://www.ims.uaf.edu/chukchi.

US Fish and Wildlife Service. 2015. Polar Bear (*Ursus maritimus*) Conservation Management Plan, Draft. US Fish and Wildlife, Region 7, Anchorage, AK.

______. 2016. Alaska Seabird Die-off. US Fish and Wildlife Service, Anchorage, AK.

US Geological Survey. 2016. USGS Current Water Data for Alaska. US Geological Survey. Accessed online at https://waterdata.usgs.gov/ak/nwis/rt.

Walkusz, W., W. J. Williams, L. A. Harwood, S. E. Moore, B. E. Stewart, and S. Kwasniewski. 2012. Composition, biomass and energetic content of biota in the vicinity of feeding bowhead whales (*Balaena mysticetus*) in the Cape Bathurst upwelling region (south eastern Beaufort Sea). *Deep Sea Research Part I: Oceanographic Research Papers* 69:25-35.

Walsh, J. E., F. Fetterer, J. Scott Stewart, and W. L. Chapman. 2017. A database for depicting Arctic sea ice variations back to 1850. *Geographical Review* 107:89-107.

Wang, M. and J. E. Overland. 2009. A sea ice free summer Arctic within 30 years? *Geophysical Research Letters* 36:L07502.

______. 2015. Projected future duration of the sea-ice-free season in the Alaskan Arctic. *Progress in Oceanography* 136:50-59.

Weeks, W. 2010. *On Sea Ice*. University of Alaska Press, Fairbanks, AK.

Weingartner, T. 2006. Circulation, Thermohaline Structure, and Cross-shelf Transport in the Alaskan Beaufort Sea. School of Fisheries and Ocean Sciences, University of Alaska Fairbanks, Fairbanks, AK.

______. 2008. Physical oceanography, *In Arctic Ocean Synthesis: Analysis of Climate Change Impacts in the Chukchi and Beaufort Seas with Strategies for Future Research*. R. Hopcroft, B. Bluhm, and R. Gradinger eds. University of Alaska Fairbanks, Institute of Marine Science, Fairbanks, AK.

Weingartner, T., E. Dobbins, S. Danielson, P. Winsor, R. Potter, and H. Statscewich. 2013. Hydrographic variability over the northeastern Chukchi Sea shelf in summer-fall 2008–2010. *Continental Shelf Research* 67:5-22.

Weingartner, T., W. Maslowski, S. Okkonen, R. Pickart, J. Trefey, and R. Woodgate. 2012. Chukchi/Beaufort physical oceanographic overview. *In* Synthesis of Arctic Research (SOAR) Workshop. Anchorage, AK.

Weingartner, T. J., K. Aagaard, R. Woodgate, S. Danielson, Y. Sasaki, and D. Cavalieri. 2005a. Circulation on the north central Chukchi Sea shelf. *Deep Sea Research Part II: Topical Studies in Oceanography* 52:3150-3174.

Weingartner, T. J., S. L. Danielson, and T. C. Royer. 2005b. Freshwater variability and predictability in the Alaska Coastal Current. *Deep Sea Research Part II: Topical Studies in Oceanography* 52:169-191.

Welch, C. 2015. Mass Death of Seabirds in Western US Is 'Unprecedented'. National Geographic, Washington, DC. Accessed online 4 April 2017 at http://news.nationalgeographic.com/news/2015/01/150123-seabirds-mass-die-off-auklet-california-animals-environment/.

______. 2016. Huge Puffin Die-off May be Linked to Hotter Seas. National Geographic, Washington, DC. Accessed online 4 April 2017 at http://news.nationalgeographic.com/2016/11/tufted-puffins-die-off-bering-sea-alaska-starvation-warm-water-climate-change/.

Woodgate, R. A., T. Weingartner, and R. Lindsay. 2010. The 2007 Bering Strait oceanic heat flux and anomalous Arctic sea-ice retreat. *Geophysical Research Letters* 37:L01602.